# Structural architecture and glacitectonic evolution of the Mud Buttes cupola hill complex, Southern Alberta, Canada

Emrys Phillips[1]*, David J A Evans[2], Nigel Atkinson[3] and Allison Kendall[4]

1. British Geological Survey, The Lyell Centre, Research Avenue South, Edinburgh EH14 4AP, UK
2. Department of Geography, University of Durham, South Road, Durham, DH1 3LE, UK
3. Alberta Geological Survey, Twin Atria Building Suite 402, 4999 - 98 Avenue, Edmonton, Alberta T6B 2X3, Canada
4. Department of Geoscience, University of Calgary ES118, 2500 University Drive Northwest, Calgary, Alberta T2N 1N4, Canada

* Corresponding author: e-mail - erp@bgs.ac.uk

## Abstract

This paper presents the results of a detailed multidisciplinary study of the deformed bedrock and overlying Quaternary sediments exposed at the Mud Buttes in southern Alberta, Canada. This large, arcuate cupola hill is composed of intensely folded and thrust sandstones, siltstones and mudstones of the Cretaceous Belly River Group. Glacitectonism responsible for the development of this internally complex landform occurred at the margin of the newly defined Prospect Valley lobe of the Laurentide Ice Sheet. Analysis of the deformation structures reveals that construction of this landform occurred in response to at least two phases of south-directed ice sheet advance separated by a period of retreat. The first phase led to the formation of a forward propagating imbricate thrust stack leading to polyphase deformation of the Belly River Group. D1 thrusting led to the detachment of thrust-bound slices of bedrock which were accreted to the base of the developing imbricate stack. This process resulted in the structurally higher and older thrust-slices being progressively “back-rotated” (tilted), accompanied by D2 thrusting and folding. Further thrusting during D3 was restricted to the core of the Mud Buttes as the deforming sequence accommodated further compression imposed by the advancing ice. Minor oscillations of the ice margin led to localised brittle-ductile shearing (D4) of the bedrock immediately adjacent to the ice contact part of the thrust stack. The second phase of ice advance led to the accretion of a relatively simple thrusted and folded sequence seen the northern side of Mud Buttes. The resulting composite thrust moraine was subsequently overridden by ice

advancing from the NNW to form a dome-like cupola-hill. This readvance of the Prospect Valley lobe led to the formation of a thin carapace of Quaternary sediments mantling the Mud Buttes which include glacitectonite, till and an organic-rich clay-silt (?palaeosol).

**Keywords:** large-scale glacitectonism, forward propagating thrust-stack model, Mud Buttes, Laurentide ice sheet.

## 1. Introduction

Large-scale glacitectonic deformation is caused as a glacier or ice sheet pushes into and overrides a pre-existing sequence of sediments and/or bedrock, and typically involves folding and thrusting. The range of structures developed is comparable to those observed within orogenic mountain belts, only at a much smaller scale. Furthermore the resultant thrust complexes are formed over significantly shorter timescales with even the largest glacitectonic moraines developing within tens to hundreds of years and even within a year at surging glacier margins. The similarity between thrust complexes formed in orogenic and glacial settings has invariably led to the application of a thin-skinned thrust model to deformed glacigenic sequences, where the deformation leads to the stacking of detached, thrust-bound slices of sediment and/or bedrock above a prominent basal décollement or sole thrust (e.g. Rotnicki, 1976; Dahlen *et al*., 1984; van der Wateren, 1985; Croot, 1987; Mulugeta and Koyi, 1987; van Gijssel, 1987; Pedersen, 1987; Aber *et al*., 1989; Harris *et al*., 1995, 1997; Williams *et al*., 2001; Andersen *et al*., 2005; Phillips *et al*., 2008; Vaughan-Hirsch and Phillips, 2016; Lee *et al*., 2013, 2016). Experimental data (e.g. sand box experiments) suggest that the structural style and geometric characteristics of proglacial thrusting are strongly controlled by the frictional properties of the sediments being deformed (Davis *et al*., 1984; Nieuwland *et al*., 2000). Consequently, several studies have suggested that the presence of low-frictional, water-rich sediments within the deforming sequence may assist thrust propagation into the foreland (van Gijssel, 1987; Andersen *et al*., 2005; Phillips *et al*., 2008; Vaughan-Hirsch and Phillips, 2016).

Glacitectonic thickening of the deforming sequence during proglacial thrusting and overriding can lead to the formation of a range of landforms such as hill-hole pairs and glacially overridden cupola hills, as well as a variety of moraines, from small-scale push features to much larger composite ridges and thrust-block moraines, which mark the former positions of ice marginal stillstands or readvances (Bluemle and Clayton, 1983; Aber *et al*., 1989; Aber and Ber, 2007; van der Wateren, 2005; Evans, 2007; Benn and Evans, 2010). The glacitectonised sequences within these landforms often contain a complex array of cross-cutting structures (folds, faults, tectonic fabrics), which record 'polyphase' deformation histories. Well-documented examples include: large-scale thrusting of sandstone and shale bedrock and glacial sediments in North Dakota (Bluemle and Clayton, 1984); thrusting and detachment of sandstone blocks in the prairie regions of Alberta and Saskatchewan, Canada (Moran *et al*., 1980); proglacial thrusting of frozen blocks of glacial outwash and marine sediments in the Canadian Arctic (Evans and England, 1991); deformed Quaternary glaciofluvial sediments within the composite ridges of the Dammer and Fürstenauer Berge region of Germany (van der Wateren, 1987; 1995); folded and thrust Cretaceous chalk bedrock and associated Pleistocene sediments on the Isle of Rügen, northern Germany (Steinich, 1972; Gehrmann *et al*., 2016) and at Fur Knudeklint and Møns Klint, Denmark (Pedersen, 2005; 2014); imbricated and folded Quaternary sediments at St. Bees, Cumbria, England (Williams *et al*., 2001), Dinas Dinlle, northwest Wales (Harris *et al*., 1997; Thomas and Chiverrell, 2007, 2011) and the Bride Moraine on the Isle of Man (Slater, 1931; Thomas *et al*., 2006; Roberts *et al*., 2006; Thomas and Chiverrell, 2011). High resolution 2D and 3D shallow offshore seismic surveys have also revealed large-scale thrust complexes (up to several hundred metres thick and kilometres across) on the formerly glaciated continental shelf surrounding northern Europe (e.g. Huuse and Lykke-Andersen, 2000; Vaughan-Hirsch and Phillips, 2016; Pedersen and Boldreel, 2016). Consequently, understanding how these glacitectonic thrust complexes are initiated and evolve and the ice sheet dynamics required for their formation is becoming increasingly important in aiding our understanding of the evolution of major palaeo ice masses.

This paper focuses upon the glacitectonised sequence exposed at the Mud Buttes in southern Alberta, Canada (Figure 1), where Cretaceous sandstones, siltstones and mudstones are intensely folded and thrust within a large-scale (c. 2 km long, c. 800 m wide), arcuate cupola hill (Hopkins, 1923; Slater, 1927; Fenton *et al*., 1993). The Mud Buttes is one of a number of large glacitectonic landforms (e.g. Neutral Hills, Misty Hills; Figure 2) in this part of Alberta (Shetsen, 1990; Fenton *et al*., 2013; Atkinson *et al*., 2014a) which are thought to have been produced during the readvance of ice streams against the northernmost extension of the NW-SE orientated Missouri Coteau escarpment during retreat of the Laurentide Ice Sheet (Evans *et al*., 2008). Although the Mud Buttes is acknowledged as a text book site for the study of glacitectonics (e.g. Aber and Ber, 2007; Benn and Evans, 2010), very little detailed research has been carried out here since the pioneering work of George Slater (Slater, 1927). The results of the multidisciplinary study (sedimentology, structural geology and geomorphology) of the Mud Buttes area presented here address this shortfall. The detailed analysis of the structures developed within this thrust complex has enabled the construction of a cross-section through the glacitectonised sequence and the establishment of a relative chronology of deformation events that took place during its construction. The factors controlling the initial detachment, transport and subsequent accretion of the thrust-bound bedrock slices are discussed, with large-scale glacitectonism being related to surge-type behaviour of lobate ice stream margins during the later stages of ice sheet recession from Alberta.

## 2. Methods

The glacial geomorphology of the study area was mapped from a 15 m light detection and ranging (LiDAR) bare-earth digital elevation model (DEM) and the Shuttle Radar Topography Mission (SRTM, 30 m DEM). This mapping was based on the non-genetic, morphometric characteristics of landforms (Figures 1b to 3) and was augmented by reference to aerial photograph mosaics flown and compiled by the Alberta Department of Lands and Forest in the 1950s as well as Google Earth imagery. This approach has been employed previously on the Canadian prairies (Evans *et al*., 2008, 2014; Ó Cofaigh *et al*., 2010; Fenton *et al*., 2013; Atkinson *et al*., 2014a, b) and ensures the representation of landform detail at a variety of scales appropriate to the study area being depicted. Genetic terms were then applied to features on the finalised map based on the descriptive and interpretative details provided below utilizing where appropriate interpretations from previous research (e.g. Shetsen, 1987, 1990; Fenton *et al*., 2013; Atkinson *et al*., 2014a and references therein).

The glacitectonic deformation of the glacial sediments and Cretaceous bedrock exposed at the Mud Buttes has been investigated using a range of macroscale techniques. The sections through the deformed bedrock were described on the basis of their macroscale features, particularly lithology, type of bedding, bed geometry and structure (both sedimentary and glacitectonic). The orientation of folds, foliations, and faults, as well as bedding were recorded at a number of localities (Figure 4) and plotted on a series of lower hemisphere stereographic projections (dip and dip-direction/azimuth) (Figures 4c to g) and rose diagrams (strike/trend) (Figure 4h) using StereoStat software by Rockworks™. The sense of asymmetry of various fold phases and movement on the faults, and inter-relationships between the various generations of structures were established. Successive generations of structures (e.g. folds F1, F2…..Fn) are distinguished using the nomenclature normally used in structural geological studies (F1 earliest folds to Fn latest). However, this nomenclature does not necessarily imply that these structures evolved during separate deformation events (D1, D2…..Dn). A series of overlapping photographs of key sections within the deformed sequence (see Figures 5 to 8) enabling the analysis of the larger-scale structures and the construction of a schematic structural cross-section through the Mud Buttes thrust complex.

Sedimentological investigations were undertaken on the Quaternary deposits that form a carapace over the non-dissected parts of the Mud Buttes. Individual lithofacies are described in detail from five locations based upon bedding, texture, lithology and sedimentary structures and classified according to the modified scheme of Eyles *et al*. (1983) proposed by Evans and Benn (2004) and Evans (in press), specifically in relation to glacigenic diamictons and glacitectonites. In order to assess the former shearing history of the sediments and potential ice flow direction, clast macrofabrics were measured based upon ≥30 clasts per sample, because clasts were too sparsely distributed to enable larger samples and at the same time ensure that data collection was confined to small areas of individual sedimentary units. Additionally, the orientations of striations/groves, located at the basal contact of a diamicton in one exposure, were measured. The macrofabrics are based on the dip and azimuth (orientation) of the clast A-axes and were measured using a compass clinometer, aiming to use predominantly clasts in the range of 30-125 mm (A-axis length) to allow comparison with other studies (Benn, 1994a, b; 1995; Evans, 2000; Evans and Hiemstra, 2005; Evans *et al*., 2007). The A-axes of clasts will tend to rotate to parallelism with the direction of shear in a shearing Coulomb plastic medium like till (c.f. March, 1932; Ildefonse and Mancktelow, 1993; Hooyer and Iverson, 2000). Fabric data were plotted in Rockware™ on spherical Gaussian weighted, contoured lower hemisphere stereographic projections. Statistical analysis of fabric data was undertaken using eigenvalues ($S_1$ – $S_3$), based on the degree of clustering around three orthogonal vectors ($V_1$ – $V_3$), and presented in fabric shape ternary diagrams (Benn, 1994b). This identifies the three end-members of predominantly isotropic ($S_1$-$S_2$~$S_3$), girdle ($S_1$-$S_2$>>$S_3$) or cluster fabrics ($S_1$>>$S_2$~$S_3$). Further analysis of strain history involved the classification of fabric data according to five modal groups (un-unimodal, su-spread unimodal, bi-bimodal, sb-spread bimodal and mm-multimodal) and their plotting against isotropy (S3/S) in a modality-isotropy template, after Hicock *et al*. (1996) and Evans *et al*. (2007).

## 3. Location of study area and regional geological context

The Mud Buttes form part of an extensive area of glacitectonic constructional terrain that comprises the core of the Neutral Hills Uplands (Pettapiece, 1986; Shetsen, 1987). Geomorphologically, at 50 m high, they are not the most spectacular features in these uplands (Figure 2), which include the much larger and sharper relief Neutral Hills (120 m), Misty Hills (85 m) and Nose Hill (100 m), but are invaluable for interpreting landform genesis because their cores are well-exposed in a badland terrain created by deglacial meltwater incision and postglacial runoff. Long recognized and mapped as glacitectonised bedrock (Hopkins, 1923; Slater, 1927; Kupsch, 1962; Moran *et al*., 1980; Shetsen, 1987, 1990; Evans *et al*., 2008), this suite of landforms is large enough to form its own physiographic zone at a regional scale (Bostock, 1970a, b; Pettapiece, 1986).

Geologically, the region is located in the south-central part of the Western Canada Sedimentary Basin and is underlain by fluvial and marine deposits associated with the transgression of the Western Interior Seaway during the Late Cretaceous (Mossop and Shetsen, 1994). The Belly River Group outcrops throughout the Mud Buttes and comprises a fluvial succession of interbedded fine to coarse-grained pale coloured (light grey to light brown) sandstone, dark coloured siltstone and mudstone with minor layers of coal and sideritic concretions (Hopkins, 1923; Slater, 1927; Fenton *et al*., 1993; Prior *et al*., 2013). These are overlain by marine strata of the Bearpaw Formation, which primarily consists of laminated mudstone, with minor sandstone beds and layers of bentonite concretions. Although the Bearpaw Formation underlies most of east-central Alberta and outcrops in the Misty Hills to the south (Slater, 1927; Fenton *et al*., 1993; Glombick, 2010), it is absent in the Mud Buttes.

## 4. Glacial Geomorphology of the Neutral Hills Uplands and surrounding areas

The Mud Buttes lie in the south-central part of the Neutral Hills Uplands, an area of complex and varied glacial landforms dominated by glacitectonic compressional structures but also containing expansive areas of hummocky terrain and kame and kettle topography (Figures 1 and 2). This area lies between the strongly streamlined trunks of the former palaeo-ice streams previously identified by Evans *et al*. (2008, 2014, 2016), Ross *et al*. (2009) and Ó Cofaigh *et al*. (2010) as 'flow set 1' and marked here on Figure 1b as the Central Alberta Ice Stream (CAIS) and Maskwa Ice Stream. Based upon the cross-cutting relationships depicted in Figure 1b (see Evans *et al*. in prep for details), it appears that the CAIS operated for longer than previously thought, maintaining a N-S flow in the west of the study region through ice flow phases 3-6. In the centre of the study region, the later ice streaming phases formed flow sets 2 and 3, which in the Neutral Hills Uplands are manifest respectively as a WNW-ESE orientated streamlined corridor that is subtle but cuts across the numerous thrust masses (flow set 2) and a multi-lobate assemblage of proglacial thrust masses (3a-c) at the southern limit of a NNE-SSW aligned streamlined trunk zone, hereby called the 'Prospect Valley lobe' (Figure 1b). The more substantial thrust masses of the Neutral Hills and Misty

Hills were similarly thought by Ó Cofaigh *et al*. (2010) to have been constructed during the formation of flow sets 2 and 3 when the ‘elbow’ of the flow set 2 ice stream was more lobate and radiating to the S and SW (Figure 1b). The impinging of the eastern margin of the CAIS also likely played a significant role in landform construction in the western part of the Neutral Hills Uplands. Based upon cross-cutting relationships, it appears that the Prospect Valley lobe created an inset sequence of thrust masses (phases/margins 3a-c), which were partially streamlined by later flow phases 4 and 5 (Figure 1b). A final readvance of the Prospect Valley lobe (phase 6) constructed an extensive area of kettled thrust masses to the north, which also appears to be linked to the construction of a hill-hole pair on the bed of the former Maskwa Ice Stream (Evans *et al*., 2016).

The southernmost, and hence oldest, of these major thrust masses appears to be the Misty Hills, which lie 25 km south of the major arc of the Neutral Hills/Nose Hill thrust moraine (Figures 2 and 3). The Misty Hills form the most prominent and dissected, likely more recently reactivated, part of a much larger arc of glacitectonised bedrock masses which sweep ESE across the Sounding Creek valley. At their geographical centre they display a variety of structural lineaments which appear to highlight individual thrust masses that have been differentially displaced or slightly rotated in the horizontal plane during glacial compression (Figure 3). Lineaments are the surface expression of the crests of large-scale fold noses or thrust faults and are clearly related to thrust masses where their internal structure is visible. Even in the absence of exposures, surface lineaments or ridges have been equated to glacitectonic compression based upon their appearance as closely spaced, parallel-aligned but often sinuous corrugations (e.g. Kupsch, 1962; Christiansen and Whitaker, 1976; Sauer, 1978; Moran *et al*., 1980; Bluemle and Clayton, 1983; Tsui *et al*., 1989). A protocol for the differentiation of such glacitectonic ridges and visually similar appearing recessional push-moraines on the prairies was developed by Evans *et al*. (2014).

The details of the structural lineaments identified in Figure 3 from the Misty Hills reveal variously orientated linear chains of depressions (interpreted as marking the traces of faults) and three prominent ridge patterns of likely folded and thrust strata: (i) N-S aligned; (ii) WSW-ENE aligned; and (iii) arcuate ridges. The N-S-trending ridge pattern is the most significant, especially in the west of the uplands, and it continues northwards through an upland spine that separates the Monitor Creek and Sounding Creek valleys. Additionally, individual thrust masses or blocks can be identified where linear depressions, likely marking fault (strike/slip) traces, demarcate their boundaries. For example, at the western-end of the Misty Hills, a large NNE-SSW aligned linear depression forms the boundary between a thrust block comprising N-S aligned ridges and another whose predominantly N-S-trending ridges have been curved into a W-E alignment; this gives the impression that the northern block has been displaced to the SSW along the linear depression or fault accompanied by the distortion of the ridge pattern by dragging the ridges (steep fold noses) northwards. Elsewhere, arcuate ridge patterns appear to lie south of domed structures that otherwise comprise WSW-ENE or N-S aligned ridges; the Mud Buttes form one such dome. Although the structurally-controlled ridge patterns can be traced into the eastern part of the Misty Hills, the topography in this area is more subdued and the landforms more hummocky and pitted, with increasingly expansive water-filled depressions in an eastward direction, culminating in the larger expanses of Misty Lake and Grassy Island Lake. Sinuous ridges (eskers) are also prominent in this area and trend W-E, winding their way between densely-spaced hummocks, flat-topped hills (prairie mounds) and circular rimmed features (donuts) (Figure 3). This landform association, hereon named the Grassy Island Moraine, is one that is traditionally related to the stagnation of debris-rich ice on the prairies (Gravenor and Kupsch, 1959; Clayton and Cherry, 1967; Clayton and Moran, 1974; Johnson and Clayton, 2003; Clayton *et al*., 2008; Evans *et al*., 2014) and demarcates an expansive area of former buried glacier ice on the eastern part of the Misty Hills through which structural lineaments are visible in some locations. Esker networks cross Grassy Island Lake, which occupies an elongate depression along the thalweg of a major preglacial river that flowed along the present Monitor Creek before turning SE to flow through the Misty Lake area (Carlson, 1969); esker continuity indicates that eastward flowing meltwater drainage was englacial, enabling water to bypass the preglacial valley, which remained inundated by ice during deglaciation, explaining why such prominent ice stagnation topography (Grassy Island Moraine) developed in this area. Both the draping of the Misty Hills structures by eskers as well as their visibility through the hummocky terrain indicate that they were overrun by glacier ice after construction.

The various alignments of lineaments described above and their relationships to regional overprinting/streamlining (Figures 1b and 3) appear to reflect a more complex constructional history for the Misty Hills than previously reported (e.g. Fenton *et al*., 1993). The N-S-aligned lineaments continue south of the Misty Hills, beyond the limit of the high relief thrust features of the Sharp Hills (Figure 2), where they can be traced beneath the streamlined terrain of flow phase 2 (Figures 1 and 2). Hence the N-S lineaments are classified as a partially overridden or fluted thrust moraine of pre-phase 2 age. This places the origins of the Misty Hills in pre-phase 2, but later modification of these lineaments appears to have been initiated during phase 3a, the southern extent of which is demarcated by their realignment (blue line on Figure 3). The Grassy Island Moraine (Figures 2 and 3) was overprinted on the eastern Misty Hills either during this phase and/or during phase 4. A more S to SSW ice flow during phase 4 was responsible for streamlining the terrain to the north of the Misty Hills and the construction and overriding of the Mud Buttes (Figures 1b and 3; Evans *et al.*, in prep).

## 5. Deformation structures and structural architecture of the Mud Buttes

Deformation of the Belly River Group at the Mud Buttes is characterised by large-scale thrusting and folding (Figures 5 to 14). This glacially deformed sequence of sandstones, siltstones and mudstones was first described by Hopkins (1923) who stated that *"the intense deformation of the beds observed at Mud Buttes and similar localities is entirely superficial and without deep-seated significance and in no way connected genetically with tectonic disturbance of the region"*. However, it was the later work of Slater (1927) that clearly demonstrated that the deformation was the result of "*ice-action*" comparing the glacitectonism seen at the Mud Buttes with that observed on the Isle of Mön, Denmark, the Isle of Rügen, Germany, and the North Norfolk coast of eastern England. In his detailed cross-sections, Slater divided the deformed sequence at the Mud Buttes into three structural zones separated by major thrust planes (Figure 15a; also see figs. 1 and 2 of Slater 1927). This subdivision was later revised by Fenton *et al*. (1993) who argued that the glacitectonised sequence could be divided into four major thrust sheets (Figure 15b; also see fig. 16 of Fenton *et al*., 1993). Thrust sheet 1 of Fenton *et al*. (1993) (zone 1 of Slater, 1927) occurs on the southern side of the Mud Buttes and is the structurally lowest and least deformed part of the sequence (Figure 15). The structurally overlying second thrust sheet (zone 2 of Slater, 1927) was described as being characterised by an increase in the degree of folding but without appreciable thrusting (Fenton *et al*., 1993). The third thrust sheet (zone 3 of Slater, 1927) occupies the central higher ground of the Mud Buttes (Figure 15) and is formed of highly folded and thrust sandstones and mudstones (Fenton *et al*., 1993). The fourth thrust sheet (not represented on the cross sections of Slater, 1927) occurs on the northern side of the Mud Buttes (Figure 15b) and was interpreted by Fenton *et al*. (1993) as having been thrust over structurally lower sheets. Fenton *et al*. (1993) concluded that the deformation was the result of ice advancing from the north with minor changes in the orientation of the folds being indicative of a locally radial ice flow.

Our re-examination of the glacitectonism at the Mud Buttes recognises that the style and intensity of deformation varies from south to north within this polydeformed sequence (c.f. Slater, 1927; Fenton *et al*., 1993). For ease of description the sequence has been divided into four NE to SW-trending 'structural domains' (Figure 4b) which internally exhibit a similar range of structures (folds, thrusts, fabrics and shear zones) and relative intensity of deformation. The boundaries between these domains correspond to major thrusts (see

Figure 4b) which truncate bedding and deformation structures developed within the underlying domain. Structural domains 1 and 2 broadly correspond to the structurally lower three thrust sheets of Fenton *et al*. (1993) and zones 1 to 3 of Slater (1927). However a zone of intense brittle-ductile shearing has been identified on the northern-side of the central higher ground of the Mud Buttes (part of the third thrust sheet of Fenton *et al*., 1993) and assigned to structural domain 3 (see below). Structural domain 4 of this study corresponds to the fourth thrust sheet of Fenton *et al*. (1993). The deformation structures present within each of these domains are described below.

### *5.1. Structural Domain 1*

Structural domain 1 occurs on the southern-side of the Mud Buttes (Figure 4b) and is characterised by a gently to moderately (10° to 45°) N to NE-dipping (Figures 4c and d) sequence of interbedded pale grey, fine-grained sandstones, siltstones and grey-brown mudstones deformed by northerly dipping (Figures 4e and f), southerly directed thrusts (Figures 5 and 6). Although the sequence has locally been repeated by thrusting, sedimentary structures (graded bedding, cross-lamination) preserved within the Belly River Group indicate that these rocks are generally the right-way-up. The thrusts are typically developed within the relatively weaker mudstones, particularly close to, or immediately adjacent to the boundaries of the thicker, more competent sandstones. Their orientation varies from bedding-parallel to moderately dipping structures which clearly truncate bedding (Figure 5a and b). Small-scale and mesoscale, asymmetrical, southerly verging folds are only locally developed within domain 1 occurring in the hanging-walls of the thrusts where they deform 1 to 2 m thick units of thinly interbedded sandstones and mudstones (Figure 5). Northwards, across domain 1, the mesoscale folds appear to tighten, with their increasingly steep southern limbs resulting in the localised overturning (towards the south) of bedding (Figure 6). Small-scale thrusts are locally observed within the hinge zones of the folds and deforming the overturned limbs of these structures (Figures 5a, 5b, 6b and 6c). In detail these small-scale thrusts vary from discrete, planar dislocations to narrow brittle-ductile shear zones possessing a well-developed S-C fabric (Figure 6d). Where developed, the geometry of this asymmetrical foliation records a southerly directed sense of shear.

### *5.2. Structural Domain 2*

Structural Domain 2 is located immediately to the north of domain 1 and is characterised by a marked increase in the occurrence of folding and thrusting within the Belly River Group (Figures 7 to 9). The relative intensity of this deformation increases from south to north across domain 2 and is accompanied by a progressive increase in the angle of dip of bedding and the thrusts (see Figures 8a, 8b and 8c). Although repeated by thrusting, bedding within the Belly River Group is only locally overturned on the steep limbs of associated meso- and large-scale folds. Both Slater (1927) and Fenton *et al*. (1993) recognised this increase in the intensity of deformation within the central part of the Mud Buttes (see Figure 15). However, detailed analysis of the relationships between the various generations of folds and thrusts present within domain 2 has revealed that within this part of the thrust complex, the Belly River Group has undergone a distinct polyphase deformation history (see below). Domain 2 is further subdivided into: (i) domain 2a located along its south side and composed of moderately inclined and thrust repeated sandstones, siltstones and mudstones (Figures 4, 5 and 6a); and (ii) domain 2b occupying the central higher ground of the Buttes and characterised by moderately to steeply inclined, highly folded and thrusted Belly River Group rocks (Figures 9c, 9d, 10 and 11). Although these two subdomains can be broadly correlated with the second and, to a lesser extent, third thrust sheets of Fenton *et al*. (1993), the progressive nature in the change in both the intensity and attitude of the deformation structures from domain 2a into domain 2b indicates that they share a common deformation history and are therefore considered to form part of the same structural domain.

Immediately adjacent to the southern boundary of domain 2a are locally well-developed large-scale, upright, tight to moderate to tight, ‘box-like’ fold structures (Figures 8b, 9a, 9b and 9c); the “*diapyre curve*” of Slater (see fig. 3 of Slater, 1927). The local truncation of bedding on the limbs and within the hinge zones of these folds indicate that they deform a set of earlier developed thrusts (T1), indicating that they are F2 in age (Figures 9a and b). The sense of offset of bedding across these earlier developed thrusts records a southward displacement during T1 thrusting. The sandstones and mudstones on the limbs of the folds are also locally deformed by a set of later thrusts (T2) and more steeply inclined reverse faults (Figures 9a and b). The sense of displacement on these relatively younger thrusts is also towards the south, indicating that both the T1 and T2 phases of faulting probably resulted from the same overall N-S-directed sense of shear (see Figures 9a and b). Locally developed northerly directed thrusts close to the southern margin of domain 2a and are interpreted as minor back-thrusts.

The dominant deformation within the remainder of domain 2a is the thrust repetition and stacking of fault-bound slices of Belly River Group (Figures 7 and 8). As noted above the dip of these thrust slices progressively increases northwards across the domain (Figure 8). The thrusts are once again preferentially developed within the weaker mudstones immediately adjacent to the boundaries with the more competent sandstone units (see Figures 8 and 9). In detail, the individual thrust planes are locally marked by thin (5 to 20 cm thick) lenses (1 to 2 m long) to laterally more extensive (5 to 15 m) layers of a dark grey, highly fissile, organic-rich mudstone with associated minor ironstone nodules (Figures 10a and b), suggesting that these peaty-looking mudstones, where present, acted as a focus for thrusting. Small-scale (centimetre scale) asymmetrical folds, asymmetrical S-C fabrics and the offset of bedding associated with the thrusts within domain 2a similarly record a consistent southerly directed sense of displacement.

Large-scale, moderately inclined synclines developed within the foot-walls of the thrusts are truncated by these low-angle faults (Figures 7a and b) and possibly represent the relicts of tip-folds developed in front of the propagating thrusts, which became dissected by these brittle structures as thrusting continued. These folds can be seen to deform both bedding and a set of earlier developed bedding-parallel thrusts (T1) (Figures 7a and b), indicating that large-scale thrusting and imbrication within domain 2a is predominantly T2 in age. Mesoscale folds within domain 2a range from relatively simple, upright to inclined, asymmetrical, south-verging, structures developed within the hanging-walls of the T2 thrusts (Figures 7c and 8c) to more complex structures with associated well-developed, small-scale S, M and Z shaped parasitic folds (Figure 9d). These more complex fold systems are typically observed deforming thinly interbedded sandstones, siltstones and mudstones, and occur within discrete bands or horizons following the outcrop pattern of the more mudstone-rich, thinly bedded units within the Belly River Group. The NNE-SSW-trending folds (Figures 4g and h) are non-cylindrical structures with curved axial traces which plunge (up to 20°) towards the E/ENE or W/WSW. They locally exhibit a marked thickening of the hinge zone and/or steeply inclined to overturned limbs, as well as attenuation (thinning) of their moderately inclined upper limbs. The folds are F2 in age and were observed deforming earlier developed low-angle (with respect to bedding) to bedding-parallel T1 thrusts. Small- to mesoscale T2 thrusts (displacements up to 1-2 m) developed within the cores of the larger F2 folds (Figure 9d) are interpreted as either accommodation structures formed in response to the progressive tightening of the folds during deformation, or the propagating tips of larger blind T2 thrusts. Both the folds and thrusts (both T1 and T2) record a sense of shear towards the south, indicating that they probably developed during the same overall southerly directed deformation event.

The boundary between domains 2a and 2b is gradational and marked by an increase in the relative intensity and scale of the folding and thrusting (Figures 11 and 12), with the largest scale (amplitude of tens of metres) occurring within the "core" of the Mud Buttes (Figure 12). Units of thinly bedded sandstone and mudstone within the Belly River Group show evidence of increased amounts of shortening with well-developed south-verging, asymmetrical to locally disharmonic folds and southerly directed thrusts (Figure 11). The folds are tight to locally isoclinal, steeply to moderately inclined, southerly verging, non-cylindrical structures which are locally dissected by moderate to steeply inclined, N/NNE-dipping thrusts (Figures 12a and b). Ductile shearing of the limbs of the isoclinal folds during folding resulted in the attenuation and localised disruption of bedding within the sandstones (see Figures 12a and b). Small- to mesoscale folds developed on the limbs of the larger folds exhibit S, M and Z geometries depending upon their position relative to the hinges of these macroscale structures (Figures 12c and d).

### *5.3. Structural Domain 3*

Structural domain 3 has been identified flanking the northern side of the higher ground within the "core" of the Mud Buttes (Figure 4). This c. 40 to 80 m wide zone of relatively intense brittle-ductile deformation (Figures 13a and b) pinches out laterally to the W and E (see Figure 4b) where it appears to have been cut out at the base of the structurally overlying domain 4 (see below). Domain 3, where present, is preferentially developed within a relatively mudstone-rich part of the Belly River Group (see Figures 13a and b). It is characterised by tight to isoclinal, southerly verging, asymmetrical rootless folds deforming 0.5 to 1.5 m thick sandstone units and highly foliated, fissile mudstones and siltstones (Figures 13a and b). The hinge zones and overturned limbs of these folds are cut by a series of small-scale, northerly dipping thrusts which have accommodated displacements from a few millimetres to several tens of centimetres. Narrow (5 to 15 cm wide) brittle-ductile shear zones deforming the sandstones, siltstones and mudstones possess a locally well-developed S-C fabric which record a relatively consistent southerly directed sense of shear (Figures 10c and d).

The boundary between domain 3 and the structurally underlying domain 2 is marked by a 5 to 10 m wide shear zone containing truncated non-cylindrical, tight to isoclinal folds deforming the sandstones (Figures 13c and d) and intense ductile shearing within the more mudstone-rich units (Figures 13c and d). The primary sedimentary lamination within the mudstones and siltstones within this shear zone has been variably transposed by a heterogeneously developed northerly dipping (69°N/291°, 66°N/300°, 71°N/292°) tectonic foliation, responsible for the marked fissility within these rocks. Moderately to steeply inclined, northerly dipping brittle thrusts within the shear zone are marked by narrow (1 to 5 cm thick) shears which locally possess a variably developed S-C fabric. These asymmetrical shear fabrics, where present, record a southerly directed sense of displacement. The shear zone marking the southern boundary of domain 3 can be traced laterally for several tens of metres across this part of the Mud Buttes where it truncates the large-scale folds (F2) within domain 2b. This relationship indicates that the relatively intense brittle-ductile shearing which characterises domain 3 largely post-dated folding within the structurally lower parts of this thrust complex.

### *5.4. Structural Domain 4*

Structural domain 4 is the most northerly of the domains identified within the Mud Buttes and has been thrust over the structurally underlying domains (cf. Fenton *et al*., 1993). It is composed of gently to moderately north-dipping stacked thrust-bound slices of Belly River Group (Figure 14). This domain is poorly exposed compared to the remainder of the thrust complex. The structurally lower parts of domain 4, where exposed, are apparently dominated by more massive, poorly bedded sandstone (Figures 14a and b). The relative intensity of glacitectonism appears to increase structurally upwards through the domain, where the thinly bedded sandstones, siltstones and mudstones are deformed by a series of south-directed gently to moderately inclined, northerly dipping thrusts and southerly verging folds (Figures 14a and b); this increase may be largely lithologically controlled. To the east, domain 4 rests directly upon folded and thrust sedimentary rocks assigned to domain 2, with the low-angle thrust contact marking the base of domain 4 clearly truncating the underlying upright to steeply inclined, large-scale (F2) folds (Figure 10e). In the central part of the Mud Buttes, domain 4 rests directly upon the highly deformed mudstone dominated sequence of domain 3 (Figures 13a and b). These relationships indicate that southerly directed thrusting, leading to the accretion of domain 4, occurred during the later stages of the development of this thrust complex and its emplacement resulted in the truncation of the older parts of this cupola hill.

## 6. Quaternary deposits at the Mud Buttes

The glacitectonically deformed bedrock at Mud Buttes was likely covered by a thin succession of Quaternary glacigenic sediment prior to their erosion into badland topography. This is evident in a number of exposures through the various horizontal butte summits and non-gullied margins of the badland exposures. Five stratigraphic sections (MBQ 1-5; Figure 4a) are reported here as representative of the Quaternary succession.

Section MBQ 1 (Figure 16) displays 0.92 m of clast-poor diamicton, with a sandy gravel interbed, overlying pale grey silty sandstone bedrock containing gypsum nodules. The lower and thicker diamicton has a dark brown clayey silt matrix but contains deformed and undeformed intraclasts of sandstone, many of which appear to be rotten bedrock rafts, and boudins and smudges of grey clay, likely originating from mudstone bedrock rafts. The term ‘mélange’ has been used to describe deformed glacial deposits comprising fragments or blocks of pre-existing rock and/or sediment set within a fine-grained matrix (the “block-in-matrix” appearance of Cowan, 1985). Cowan (1985) recognized four types of mélange which record the progressive disruption of originally stratified sequences during deformation. In Types I (least deformed) and II the originally stratified nature of the pre-existing sediments and/or bedrock can still be recognised. In a Type III mélange the original stratification has been highly disrupted resulting in a distinctive chaotic, "block-in-matrix" appearance (Cowan, 1985). In the highly deformed Type IV mélange the bedded nature of the sediments has been overprinted. Although classified as a massive diamicton (Dmm), the appearance of the diamicton exposed within section MBQ1 is consistent with a Type III mélange of Cowan (1985). The lower and upper diamictons are separated by a 0.12 m thick unit of highly contorted and attenuated sand and fine gravel lenses (Figure 16). The boundaries of this highly deformed unit are irregular and interdigitated with the diamictons. The internally complex nature this unit is indicative of shearing occurring during emplacement of the upper diamicton. The section is capped by a 0.3 m thick clay-rich, massive, matrix-supported diamicton with an indurated but crumbly structure and containing numerous gypsum nodules.

Section MBQ 2 (Figure 17) displays a vertical continuum of well-exposed, deformed and sheared mudstone capped by a poorly exposed, clay-rich diamicton. Although the diamicton, which is the lateral equivalent of the diamictons identified in the other four sections, is not well-exposed here. However, section MBQ 2 is important in that it provides the thickest exposure through the boundary zone between Cretaceous bedrock and the overlying Quaternary sediments at Mud Buttes. The initially gently dipping (15° to 20° northwards) bedding within the mudstone bedrock becomes increasingly deformed upwards through the section (see Figure 17). This deformed sequence is c. 1.1 m thick and characterised by recumbent, tight to isoclinal, rootless to disharmonic folding of primary bedding preserved within the mudstone (Figure 17a). In the upper 0.4 m, bedding becomes increasingly disrupted and deformed by a series of southerly-verging, asymmetrical folds associated with southerly directed, small-scale thrusts and shears. This folded and thrust mudstone is truncated by the base of a 0.15 to 0.2 m thick sequence of weakly layered, predominantly grey mudstone mélange (Type IV mélange of Cowan, 1985). This friable and crumbly mudstone mélange contains small boudins and lenses of yellow and pale grey (colour reflecting subsequent alteration of mudstone by percolating groundwater) mudstone that can be seen forming more continuous beds within the less disturbed (deformed) mudrocks beneath. The weakly layered/foliated mudstone passes abruptly upwards into c. 1.1 to 1.3 m of structureless, extremely friable and crumbly mudstone in which primary bedding is absent (Figure 17b). The massive, homogeneous appearance of this mudstone (Figure 17b) is therefore interpreted as being a result of intense glacitectonic deformation which led to the overprinting of primary bedding. The initial stages of this process are represented by the structurally underlying folded and thrusted mudstone (Figures 17a and b). As deformation progressed bedding and earlier developed folds would have been progressively transposed to form a gently north-dipping glacitectonic foliation (Figure 17c). Consequently section MBQ 2 is interpreted as representing a vertical continuum typical of glacitectonite-subglacial till sequences from which clay-rich and clast-poor glacigenic diamictons (tills) are derived *in situ* from sheared bedrock (Banham, 1977; Pedersen, 1989; Hiemstra *et al*., 2007).

Section MBQ 3 (Figure 18) comprises 2.2 m of mélange and diamicton directly overlying silty sandstone upon which striated shield boulders and cobbles are lodged to form a discontinuous clast pavement or line, with striated facets bevelled at the same level as the bedrock surface (Figure 18b ii). The surface of the bedrock is also striated, manifest as prominent straight to weakly curved grooves (≤ 8 mm wide; Figure 18b iii) cut into the bedrock surface, which like the clast surface striae are strongly aligned NNW-SSE and appear to terminate at small sandstone particles. Directly overlying this striated bedrock surface is 0.5 to 1.0 m of clayey-silt diamicton containing numerous rotten sandstone intraclasts and deformed sand lenses or boudins (Figure 18a). In the basal 0.3 m, the clasts and lenses/boudins are relatively small and highly attenuated, often constituting smudges of ingested material within the diamicton matrix. They also form discrete lines that are spaced between 5 to 10 cm apart (Figure 18b ii), giving the impression of a Type IV mélange (Cowan, 1985). In the upper 0.7 m the diamicton contains larger sand lenses and boudins in which stratification is common but displays significant deformation (Figure 18b i), giving the material the appearance of a Type III mélange (Cowan, 1985) but with little sense of shearing direction. This mélange is overlain by a further 0.6 m of heterogeneous diamicton comprising crudely horizontally bedded sands, sandy gravels, silts and clay with layers of massive, clay matrix-supported diamicton, all of which have been well to very highly deformed, comparable to a Type III–Type IV mélange (Cowan, 1985). The section is capped by 0.6 m of clay-rich massive, matrix-supported diamicton comprising material that appears mudstone-rich and blocky in structure with copious gypsum nodules. The basal 0.3 m of the Type IV mélange is typical of highly sheared subglacial tills in which rafts have been plucked or cannibalised from the bedrock substrate and then highly attenuated through shearing in the subglacial traction zone and thickened incrementally to form stacked or repeated diamicton units. This origin is consistent with the lodging of shield clasts and striating of the clast facets and silty sandstone bedrock surface by small sandstone clasts, which created sole casts as they were dragged across the substrate by ice flowing from the NNW. The overlying diamictons display, firstly exhibit an apparent overall decrease in the relative intensity of deformation, manifest in a Type III mélange (Cowan, 1985) containing lenticular to irregular intraclasts of deformed (folded, faulted) stratified sand (Figures 18a and 18b i). This mélange passes upwards into to more highly deformed diamicton containing small, highly attenuated (sheared) sand lenses (Figure 18a) typical of a Type IV mélange (Cowan, 1985). A further important characteristic is the increase in stratified sands and gravels up the sequence before the emplacement of the massive clay-rich diamicton; this is interpreted as the down-ice advection of increasing volumes of stratified sediment into an incrementally thickening subglacial deforming layer forming on the northern side of the Mud Buttes. The capping clay-rich diamicton records the termination of advection and the emplacement of mudstone-dominated matrix, reflecting a change in subglacial source materials.

Section MBQ 4 (Figure 19) is a significant exposure because it contains evidence of non-glacial Quaternary deposits lying between the glacitectonically deformed bedrock and surficial glacigenic materials. These comprise 15 to 20 cm of weakly laminated to massive clayey-silt directly overlying friable mudstone, grading into ≤ 40 cm of organic-rich clayey-silt. Pollen extracted from the organic-rich material (Table 1) is well-preserved and of Quaternary age. It is predominantly indicative of a cool environment, especially in relation to the occurrence of *Artemisia*, *Chenopodiaceae*, grasses and sedges, and the appearance of boreal species such as pine, spruce and tsuga, with only hazel being relatively thermophilous. Based upon this evidence it appears that this stratigraphic unit is a palaeosol, probably a prairie-type Chernozem. This has been developed in a weakly laminated clayey-silt whose origin is uncertain but is most likely a locally derived aeolian deposit. The *in situ* nature of this palaeosol is difficult to ascertain, especially as the clayey-silt laminations in which it is developed appear to have been deformed, and therefore its status as an isochronous surface versus a glacitectonic raft is uncertain and requires further research.

The potential palaeosol is truncated but not significantly eroded by a 0.15 to 0.2 m thick, clay-rich brown diamicton (Dmm) containing deformed but laterally continuous sand lenses as well as wisps or smudges, giving the appearance of a Type II mélange (Cowan, 1985). This grades abruptly into a 0.25 m thick, massive, matrix-supported diamicton, which has a banded appearance due to numerous changes of colour from grey to brown and red-brown in undulatory and discontinuous, sub-horizontal bands. This pseudo-lamination appears to be a product of the attenuation and immature mixing of different clay-rich or sand-rich materials in a shearing medium, likely derived from the underlying mélange as a result of subglacial cannibalisation and traction zone deformation. The section is capped by 0.55 m of grey, clay matrix-supported diamicton with deformed sand lenses (Figure 19) and a fissile to crumbly texture due to the mudstone derived matrix. The measurement of a macrofabric was possible in this unit because it contains a relatively high concentration of clasts. This displays a strong alignment towards the NNW, with a mean lineation azimuth of 335° and an $S_1$ eigenvalue of 0.63 (Figure 16). In terms of its shape (Figure 20a) and modality/isotropy characteristics (Figure 20b), this macrofabric is spread-unimodal and compatible with subglacial tills with high lodgement components. The origins of the deformed lenses are unclear but are likely deformed rafts because their sandy character is unlike the clay matrix of the surrounding diamicton. Together, the Type II mélange, banded diamicton and grey diamicton are interpreted as a vertical continuum typical of a glacitectonite-subglacial till sequence from which a sheared clay-rich diamicton with deformed rafts and erratic clasts (subglacial traction till) has been derived *in situ* from the mixing of sheared mudstone and pre-existing stratified sands (Banham, 1977; Benn and Evans, 1996; Evans *et al*., 2006; Evans, in press). The glacigenic origin of this sequence documents ice advance across the glacitectonised bedrock of the Mud Buttes, indicating that two phases of glacial activity are recorded at the site with only the second phase providing evidence that the Mud Buttes were glacially overrun.

At Section MBQ 5 (Figure 21), 1.25 m of Quaternary sediment overlies a 0.2 m deformed zone developed along the Cretaceous bedrock unconformity. This deformed zone resembles a Type III mélange (Cowan, 1985) due to its heavily contorted stratified sediments comprising laminated silts, sands and clays, along with pockets of organic material and a coherent block of sandstone. Sub-rounded to sub-angular, slab-shaped sandstone boulders are embedded or lodged into this deformed zone, exhibiting A/B plane surfaces accordant with the boundary of the overlying diamicton; these boulders also form a clast line or weakly developed pavement. This is overlain by 0.65 m of massive, matrix-supported, clayey-silt diamicton with numerous rotten sand clasts and sandy lenses or boudins arranged in horizontal lines, together with short, discontinuous sand stringers or wisps spaced 5-10 cm apart, thereby resembling a Type III-IV mélange. A clast macrofabric from this diamicton displays a weak cluster, dipping NW with a mean lineation azimuth of 347° and an $S_1$ eigenvalue of 0.52 (Figure 21). In terms of its shape (Figure 20a) and modality/isotropy characteristics (Figure 20b), this macrofabric is multi-modal and typical of low shear strains, however, the weakly developed orientation is entirely compatible with the other macrofabric and striae evidence collected from, and in association with, the diamictons (tills) in other sections. The characteristics of this Type III-IV mélange are similar to those of highly sheared subglacial tills in which rafts have been plucked or cannibalized from the bedrock substrate and then highly attenuated through shearing in the subglacial traction zone by ice flowing from the NW and then thickened incrementally to form stacked or repeated diamicton units. This is consistent with the boulder line, which is likely the product of clasts being dragged through stratified materials and organics before being lodged in a Type III mélange or mixed sediment and bedrock glacitectonite. The capping 0.6 m of diamicton is poorly exposed at this site but generally comprises a clay-rich, massive, matrix-supported diamicton with a fissile to blocky structure.

In summary, the Quaternary deposits and structures identified in the five sections comprise a vertical sequence of locally preserved palaeosol and/or deformed bedrock and stratified sediments overlain by glacitectonite (sediment or bedrock derived) and/or subglacial traction till emplaced during glacier overriding from the NNW. A composite summary of the vertical logs with genetic facies codes for the Quaternary stratigraphic sequence at Mud Buttes is presented in Figure 22. In all outcrops, the clay-rich nature of the capping till indicates that mudstones were being cannibalised during later stages of glacier overriding, a process that is well represented by section MBQ 2, but this is in contrast to the exploitation of stratified sands and rare gravels (and possibly soil/organics at MBQ 5) that took place during the earlier emplacement of lower tills and glacitectonites. The distinct vertical colour change from brown to grey within the tills and glacitectonites also attests to the cannibalization of pre-existing stratified sediments and potentially also a more extensive palaeosol during early glacier overriding. Explanations of the origins of this material and the reasons for their exhaustion and replacement by local mudstone matrix during glacier overriding likely relate to the topography of the pre-advance landscape. However, it is clear that the Mud Buttes were initially constructed proglacially and later overrun by glacier ice to form the glacitectonite/till carapace, and hence they constitute a cupola hill (*sensu* Aber *et al*., 1989). Stratified sediments evident in the heavily fragmented and deformed rafts of the lower glacitectonite/till were likely excavated from the proximal depression created by the construction of the Mud Buttes as a hill-hole pair, a depression in which waterlain sediments could have accumulated during the intervening non-glacial interval. Exhaustion of this sediment supply, as well as most of the palaeosol, by glacier excavation and glacitectonite construction resulted in the subglacial removal of freshly exposed mudrocks in order to maintain till continuity and thereby seal the sequence with clay-rich till.

## 7. Discussion

It is clear from the above description that the deformation within all four structural domains occurred in response to southerly directed shear, consistent with glacitectonism at the Mud Buttes having been driven by ice advancing from the north (c.f. Fenton *et al*., 1993). The relationships between the various folds and thrusts present within domain 2 have allowed a relative chronology of deformation events to be established for at least the southern and central parts of the Mud Buttes. This progressive, southerly directed, polyphase deformation history can be divided into three main phases. The earliest phase, D1, characterised by low-angle to bedding-parallel thrusting (T1) and relatively minor folding (F1) which probably resulted in the initial detachment of the thrust slices of bedrock and shortening of the sedimentary sequence; Phase 2 leading to continued thrusting (T2) and the main phase of folding (F2) within the Mud Buttes. D1 is thought to have been largely responsible for the imbrication of the detached thrust-bound slices of Belly River Group and the main phase of "construction" within the developing composite thrust moraine. During the second phase of deformation (D2), the earlier developed T1 thrusts were locally folded by the developing F2 folds. Elsewhere, these T1 thrusts probably continued to move (i.e. evolving into T2 structures) accommodating further D2 shortening in response to compression imposed by the advancing ice. The final phase, D3, led to continued thrusting within the Belly River Group. Movement along the earlier T2 thrusts resulted in their continued propagation upwards through the sequence leading to deformation of F2 folds. Importantly, this polyphase deformation sequence has not been recognised within domains 1 and 4; these domains appear to have only encountered the equivalent to D1 in their deformation history.

The deformation structures which characterise structural domains 1, 2 and 3 record an overall increase in the intensity of thrusting and folding northwards across the Mud Buttes. This is accompanied by the progressive increase in the angle of dip of individual thrust slices of the Belly River Group, which become steeply northerly dipping within the central part of this composite thrust moraine. This relationship is illustrated in Figure 23. As noted above, the vergence of the folds and sense of displacement on the thrusts within all four structural domains indicates that deformation resulted from ice advancing from the north. The style and relative intensity of the deformation within domain 4, however, is reminiscent of that observed within parts of domain 1 (see Figure 23), marking a relative decrease in the intensity of deformation in the apparently ice-proximal part of the thrust mass where glacitectonism would be expected to be most intense. Consequently, any model explaining the structural evolution of the Mud Buttes cupola hill must take these spatial variations in the complexity and relative intensity of deformation into account (see below).

### *7.1. Glacitectonic model for the evolution of the Mud Buttes*

The structural architecture of the Mud Buttes is illustrated in Figure 23 and can be interpreted as recording the progressive increase and subsequent decrease in the relative intensity and complexity of deformation (folding and thrusting) from south to north across this glacitectonic landform. The main thrusts identified in the surface exposures have been projected downward through the Belly River Group where they are thought to link into a subhorizontal or gently north-dipping décollement surface. This décollement surface separates the allochthonous sequence of thrusted and folded sandstones, siltstones and mudstones from the structurally underlying *in situ* (autochthonous) undeformed units of the

Belly River Group. However, the depth to this basal detachment is currently unknown. The bedding-parallel to gently northerly dipping nature of the earlier (T1) thrusts can be used to suggest that this basal detachment, or sole thrust, also occurs at a low-angle within the Belly River Group.

It is clear from Figure 23 that the overall structure of the main part of the Mud Buttes (represented by domains 1, 2 and 3) is a broadly fan-shaped imbricate thrust stack. The progressive increase in dip of the individual thrust-bound slices of Cretaceous bedrock from south to north within this proposed imbricate stack is a direct result of the progressive forward propagation of the evolving composite thrust moraine (Figure 24). This forward propagation was driven by ice advancing from the north as indicated by the southerly directed sense of thrusting/shear recorded by the deformed Belly River Group. As one thrust-bound segment began to “stick” and the thrust at its base propagate (ramp) upwards through the deforming sequence, the basal décollement continued to propagate further into the forefield (Figure 24). This eventually led to the detachment of a relatively younger, structurally lower thrust slice that is accreted to the base of the evolving imbricate stack. Unless folded, these detached blocks of Belly River Group remained the right-way-up, younging toward the north. As the process of accreting successively younger (structurally) thrust-slices to the base of the developing imbricate thrust stack continued, the structurally higher and older thrust-slices are progressively “back-rotated” (i.e. the sense of rotation of the detached thrust-bound slab is towards the advancing Prospect Valley lobe) becoming increasingly steeper in attitude (Figure 24).

During back-rotation, the earlier small-scale thrusts (T1) within the thrust-blocks were folded (F2), and the hinges and overturned limbs of F1 folds cut by relatively later T2 thrusts, leading to the observed polyphase deformation history identified within domain 2. As a direct result of the forward propagation of the thrust stack, progressive back-rotation and internal deformation of the detached thrust-slices, deformation within the imbricate stack becomes progressively older and more complex towards the north and the margin of the advancing ice sheet. As a direct consequence of this process, the polyphase deformation history recorded by the Belly River Group is diachronous, with each phase becoming progressively younger towards the south (see Figure 23). D1, which is dominated by thrusting, can be equated to the initial detachment and low-angle stacking of the thrust-slices. It therefore migrated southwards to accompany the forward propagation of the imbricate thrust stack (Figure 24). D2 folding and thrusting then took over as the detached thrust-slices back-rotated and become displaced upwards as the developing imbricate thrust stack accommodated further shortening of the Cretaceous bedrock (Figure 24). D2 will also migrate southwards as new thrust-slices are progressively accreted to the base of the developing imbricate stack and are back-rotated. As a consequence of the back-rotation and up-thrusting of these detached blocks during D2, the surface topography of the evolving composite thrust moraine would have become more pronounced (see Figure 24). D3 is typically restricted to the core of the Mud Buttes and probably occurred as the sequence attempted to accommodate further compression imposed by the advancing ice. However, the restricted nature of D3 may possibly indicate that it occurred during, or shortly before the cessation of the forward propagation of the imbricate thrust stack. Consequently, this stage of the deformation history may record the “locking up” of the imbricate thrust stack and potential localised stalling of the advance of the Prospect Valley lobe.

In this relatively simple forward propagating imbricate thrust stack model, the intense brittle-ductile shearing that characterises structural domain 3 can be interpreted as having occurred in an ice-proximal position. Furthermore, these highly deformed sedimentary rocks may represent the former ice contact part of the landform. The brittle-ductile shear zone at the base of domain 3 cross-cuts and modifies earlier structures within domain 2, suggesting that this deformation may have post-dated the main constructional phase of the Mud Buttes imbricate thrust stack and is therefore D4 in age. Consequently, it is possible that the intense shearing within domain 3 records the repeated basal shear of the ice sheet up against this ice contact zone whilst the ice occupied the marginal position represented by the imbricate thrust stack.

The return to simple thrusting and folding within structural domain 4 is thought to record the accretion of a relatively younger and much smaller thrust-block moraine onto the up-ice side of the much larger imbricate thrust stack forming the bulk of the Mud Buttes (Figure 24). Forward propagation and evolution of this moraine would have been impeded by the presence of the much larger glacitectonic landform immediately down ice. The tight, box-like folding observed at the southern margin of domain 2a may have occurred during the accretion of domain 4 onto the up-ice side of the earlier formed imbricate thrust stack. Shear transmitted into the imbricate during the over-thrusting of domain 4 may have led to the localised tightening of earlier developed folds and renewed (minor) movement along pre-existing thrusts, thereby representing D5 within the main part of the Mud Buttes composite thrust moraine. This postulated minor “reactivation” of D1/D2 structures within the earlier formed imbricate thrust stack was apparently focused along the boundary between domains 1 and 2a (see Figures 23 and 24).

In summary, the construction of the Mud Buttes requires at least three phases of south-directed ice sheet advance separated by a period of retreat (Figure 24). The first phase of advance was responsible for the construction of the large imbricate thrust stack (domains 1 and 2) which underlies the main part of the Mud Buttes. Minor oscillations of the ice margin whilst it occupied this position may have locally resulted in the brittle-ductile shearing of the Cretaceous bedrock (domain 3) immediately adjacent to the ice contact part of the mass. The Prospect Valley lobe subsequently retreated northwards, only to readvance southwards once again, accreting a much smaller thrust block (domain 4) onto the up-ice side of the earlier formed (phase 1) and much larger glacitectonic landform. The presence of a palaeosol separating the glacitectonised bedrock from the overlying carapace of subglacial traction till and glacitectonite which mantles the entire Mud Buttes, if it is *in situ*, clearly indicates that these subglacial deposits record a separate (younger) ice advance across this feature (Figure 24). Alternatively, the palaeosol may itself have been emplaced as a raft and the hence the stratigraphic integrity of this material in the region requires further study. Stratified sediments within the heavily fragmented and deformed rafts of the lower glacitectonite/till were likely excavated from the proximal depression created by the construction of the Mud Buttes as a hill-hole pair, a depression in which waterlain sediments accumulated during the intervening non-glacial interval. Removal of these sediments, as well as at least most of the palaeosol, occurred during the later ice advance which resulted in the modification of the morphology of the pre-existing composite thrust moraine and the formation of a dome-like cupola-hill accompanied by the formation of the carapace of glacitectonite and till beneath the overriding ice.

### *7.2. Regional glaciological context of the Mud Buttes and factors controlling thrusting of the Cretaceous bedrock*

As noted above, the Mud Buttes along with the Neutral Hills, Misty Hills and Nose Hill form part of a large, regionally extensive assemblage of glacitectonic landforms (Figures 1 and 2) relating to ice stream marginal readvance in southern Alberta (Evans *et al*., 2008; Ó Cofaigh *et al*., 2010). The Misty Hills form the southernmost and oldest of these thrust masses (Figure 2). Fenton *et al*. (1993) suggested that initial detachment of the glacitectonised units of the Bearpaw Formation during the construction of the Misty Hills thrusting along the contact between this mudstone-rich marine sequence and the underlying Belly River Group (Mossop and Shetsen, 1994) (see fig. 14 of Fenton *et al*., 1993). This would have resulted in the effective "stripping" of the younger Bearpaw Formation from the top of the bedrock sequence, exposing the underlying (older) Belly River Group which was glacitectonically "excavated" during the construction of the Mud Buttes. This proglacial setting indicates that development the Mud Buttes resulted from a younger readvance(s) relative to the W-E flowing, pre-2 flow phase ice responsible for thrusting within the Misty Hills (Figures 1b and 3). This indicates that the initial detachment and subsequent removal of thrust-bound slabs of bedrock responsible for construction of the Misty Hills and Mud Buttes were initiated by the same substrate conditions and driving forces across the same geographical area during subsequent phases of ice sheet readvance. Sedimentary evidence presented here clearly demonstrates that the Mud Buttes thrust complex was constructed and subsequently overridden by an entirely separate and much younger readvance (flow phase 4; Figures 1b and 3). **If** the palaeosol is *in situ* rather than a raft, then overriding of the Mud Buttes by this later ice flow was preceded by a prolonged ice-free interval that enabled soils to develop across the pre-Late Wisconsinan land surface (Figure 24).

Although the Bearpaw Formation-Belly River Group boundary was the most likely focus for thrusting during the construction of the Misty Hills, the factors controlling the development of a major décollement surface associated with the development of the Mud Buttes remain uncertain. It is clear that the force exerted by the advancing ice sheet margin was transmitted into the Belly River Group, with thrusting being partitioned into the weaker mudstones (Figures 5, 7, 8). Thin lenses of peaty looking mudstone exposed along the thrust planes (Figures 10a and b) suggest that thrust propagation may have facilitated along these highly fissile sedimentary rocks. Although some early models argued for the detachment and transport of bedrock blocks (rafts) as a result of their being frozen to the base of the advancing (cold-based) ice (Banham, 1975; Aber, 1988), the structural architecture of the Mud Buttes clearly indicates that they formed as a result of proglacial to ice-marginal thrusting (Figure 24).

A number of studies have argued that proglacial to ice marginal thrusting, including the detachment of bedrock rafts in the sandstone of North Dakota (Bluemle and Clayton, 1983) and the chalk of North Norfolk, UK (Vaughan-Hirsch *et al*., 2011, 2013), can be facilitated by the introduction of pressurised meltwater along evolving thrust planes (Bluemle and Clayton, 1983; Ruszczynska-Szenajch, 1987, 1988; Phillips *et al*., 2008; Phillips and Merritt, 2008; Burke *et al*., 2009). It has been demonstrated that the periodic over-pressurisation of subglacial meltwater systems can lead to hydrofracturing and the introduction of pressurised meltwater (and sediment) into the substrate (Rijsdijk *et al*., 1999; van der Meer *et al*., 2009; Kjaer *et al*., 2006; Phillips *et al*., 2012). However, hydrofracturing on a scale required to promote the large-scale thrusting observed at Mud Buttes (and elsewhere within the Misty Hills, Neutral Hills and Sharp Hills) would have resulted in significant disruption of the Cretaceous bedrock, evidence of which is not apparent in the field (Figures 5 to 14). Alternatively, Vaughan-Hirsch and Phillips (2016) suggested that the décollement surface at the base of 5 to 6 km wide (maximum thickness 100 to 120 m) imbricate thrust stack which deforms the Aberdeen Ground Formation of the central North Sea formed in response to over-pressurisation of the groundwater system during rapid ice sheet advance (surge-type behaviour). This would result in a marked increase in the hydrostatic gradient, forcing groundwater from beneath the ice sheet (higher overburden pressure) into its forefield (lower pressure) (Boulton and Caban, 1995). A similar model could potentially be applied to the Mud Buttes where surge-type behaviour could lead to a rapid readvance of parts of the Laurentide Ice Sheet margin (Prospect Valley lobe; Figure 1b) and pressurisation of groundwater within the underlying Cretaceous bedrock. The resultant increase in water pressure within the Belly River Group could have led to fracturing of the relatively weaker mudstones, lowering their cohesive strength, leading to failure and the potential propagation of several water-lubricated detachments out into the forefield. Once formed, these detachments (bedding-parallel thrusts) would have represented ideal fluid pathways, helping to further transmit pressurised water into the forefield, thereby facilitating the forward propagation of the developing imbricate thrust-stack.

## 8. Conclusions

The Mud Buttes is one of a number of large-scale glacitectonic landforms (Neutral Hills, Misty Hills) located in southern Alberta, Canada which formed as a result of deformation occurring during ice stream marginal readvance during the overall retreat of the Laurentide Ice Sheet. This large-scale (c. 2 km long, c. 800 m wide) arcuate cupola hill is composed of intensely folded and thrusted sandstones, siltstones and mudstones of the Cretaceous Belly River Group. A detailed study of the geomorphological setting, structural geology and sedimentology of the Quaternary sediments which overlie the Mud Buttes have revealed that glacitectonism responsible for the evolution of this internally complex landform occurred at the margin of the newly defined Prospect Valley glacier lobe of the Laurentide Ice Sheet.

Analysis of the structures within the Mud Buttes clearly indicate that glacitectonism responsible for its construction involved at least three phases of south-directed ice sheet advance separated by a period of retreat. The first phase of advance led to the construction of a large, forward propagating imbricate thrust stack which underlies the main part of the Mud Buttes. The polyphase deformation history recorded by the Belly River Group within this imbricate stack is diachronous, with each phase becoming progressively younger towards the south. Low-angle to bedding-parallel D1 thrusting during the early stage of ice sheet advance led to the detachment of the thrust-bound bedrock slices and initial shortening of the Belly River Group. As successively younger (structurally) thrust-slices were accreted to the base of the developing imbricate stack, the structurally higher and older thrust-slices were progressively “back-rotated” (tilted). This tilting was accompanied by D2 thrusting and the main phase of folding to have affected the Belly River Group. Continued thrusting during D3 was restricted to the core of the Mud Buttes as the deforming sequence attempted to accommodate further compression imposed by the advancing ice. Minor oscillations of the ice margin led to localised brittle-ductile shearing (D4) of the Cretaceous bedrock on the ice contact part of the thrust stack. The second phase of ice sheet advance was responsible for the accretion (D5) of the relatively simple thrust and folded sequence of Belly River Group onto the northern side of Mud Buttes. This was accompanied by the localised Group of the earlier developed thrusts and minor box-like folding within the earlier formed imbricate thrust stack.

The glacitectonic landform left by these earlier phases of ice advance was subsequently overridden by the Prospect Valley lobe advancing from the NNW. The presence of a palaeosol (if *in situ*) separating the glacitectonised bedrock from the overlying carapace of subglacial traction till and glacitectonite may tentatively be used to suggest that these subglacial deposits record a separate (younger) ice advance. Rafts of stratified sediments the lower glacitectonite/till are thought to have been excavated from the proximal depression created by the construction of the Mud Buttes as a hill-hole pair, a depression in which waterlain sediments accumulated during the intervening interval. Removal of these sediments, as well as at least most of the palaeosol, occurred during the later ice advance which resulted in the modification of the morphology of the pre-existing thrust block moraine and the formation of a dome-like cupola-hill.

## 9. Acknowledgements

ERP publishes with the permission of the Executive Director of the British Geological Survey, Natural Environmental Research Council. The authors would also like to thank Carol Cotterill for her constructive comments on an earlier version of this manuscript. Thanks to Jim Innes in the Geography Department, Durham University for identifying the pollen in the palaeosol at Mud Buttes and Ben Hathway (Alberta Geological Survey) for advice on the regional bedrock stratigraphy. The anonymous second referee is also thanked for their constructive review.

## 10. References

Aber, J.S. 1988. Ice-shoved hills of Saskatchewan compared with Mississippi Delta mudlumps - implications for glaciotectonic models. In: Croot, D. (Ed.), Glaciotectonics: Forms and Processes. Balkema, Rotterdam, 1-9.

Aber, J.S., Ber, A. 2007. Glaciotectonism. Development in Quaternary Science 6, Elsevier, Amsterdam.

Aber, J.S., Croot, D.G., Fenton, M.M. 1989. Glaciotectonic Landforms and Structures. Kluwer, Dordrecht.

Andersen, L.T., Hansen, D.L., Huuse, M. 2005. Numerical modelling of thrust structures in unconsolidated sediments: implications for glaciotectonic deformation. Journal of Structural Geology 27, 587-596.

Atkinson, N., Utting, D.J., Pawley, S.P. 2014a. Glacial Landforms of Alberta. Alberta Geological Survey, AER/AGS Map 604.

Atkinson, N., Utting, D.J., Pawley, S.P. 2014b. Landform signature of the Laurentide and Cordilleran ice sheets across Alberta during the last glaciation. Canadian Journal of Earth Sciences 51, 1067-1083.

Banham, P.H. 1975. Glaciotectonic structures: a general discussion with particular reference to the contorted drift of Norfolk. In: Wright, A.E., Moseley, F. (Eds.), Ice Ages: Ancient and Modern. Seel House Press, Liverpool, 69-84.

Banham, P.H. 1977. Glaciotectonites in till stratigraphy. Boreas 6, 101-105.

Benn, D.I. 1994a. Fluted moraine formation and till genesis below a temperate glacier: Slettmarkbreen, Jotunheimen, Norway. Sedimentology 41, 279–292.

Benn, D.I. 1994b. Fabric shape and the interpretation of sedimentary fabric data. Journal of Sedimentary Research A 64, 910–915.

Benn, D.I. 1995. Fabric signature of till deformation, Breiðamerkurjökull, Iceland. Sedimentology 42, 735–747.

Benn, D.I., Evans, D.J.A. 1996. The interpretation and classification of subglacially-deformed materials. Quaternary Science Reviews 15, 23–52.

Benn, D.I., Evans, D.J.A. 2010. Glaciers and Glaciation. Hodder Education, London.

Bluemle, J.P., Clayton, L. 1983. Large-scale glacial thrusting and related processes in North Dakota. Boreas 13, 279-299.

Bostock H.J.1970a. Physiographic regions of Canada. Geological Survey of Canada Map 1254A, scale 1:5 000 000.

Bostock H.J. 1970b. Physiographic subdivisions of Canada. In: Douglas R.J.W. (ed.), Geology and Economic Minerals of Canada. Geological Survey of Canada, Economic Geology Report 1, 11-30.

Boulton, G.S. and Caban, P. 1995. Groundwater flow beneath ice sheets, part II; It's impact on glacier tectonic structures and moraine formation. Quaternary Science Reviews 14, 563-587.

Burke, H., Phillips, E., Lee, J.R., Wilkinson, I.P. 2009. Imbricate thrust stack model for the formation of glaciotectonic rafts: an example from the Middle Pleistocene of north Norfolk, UK. Boreas 38, 620-637.

Carlson, V.A. 1969. Bedrock topography of the Oyen map area NTS 72M, Alberta. Research Council of Alberta, 1:250,000 scale map.

Christiansen, E.A., Whitaker, S.H. 1976. Glacial thrusting of drift and bedrock. In Leggett, R. F. (ed.): Glacial Till, 121–130. Royal Society of Canada, Special Publication 12.

Clayton, L., Cherry, J.A. 1967. Pleistocene superglacial and ice walled lakes of west-central North America. North Dakota Geological Survey, Miscellaneous Series 30, 47–52.

Clayton, L., Moran, S.R. 1974. A glacial process-form model. In: Coates, D.R. (ed.): Tills and Glaciotectonics, 183–195. A. A. Balkema, Rotterdam.

Clayton, L., Attig, J.W., Ham, N.R., Johnson, M.D., Jennings, C.E., Syverson, K.M. 2008. Ice-walled-lake plains: implications for the origin of hummocky glacial topography in middle North America. Geomorphology 97, 237–248.

Cowan, D.S. 1985. Structural styles in Mesozoic and Cenozoic mélanges in the western Cordillera of North America. Geological Society of America Bulletin 96, 451-462.

Croot, D.G. 1987. Glaciotectonic structures: a mesoscale mode of thin-skinned thrust sheets? Journal of Structural Geology 9, 797, 808.

Dahlen, F., Suppe, J., Davis, D. 1984. Mechanics of fold-and-thrust belts and accretionary wedges: Cohesive Coulomb theory. Journal of Geophysical Research 89, 10087–10101.

Davis, D., Suppe, J., Dahlen, F.A. 1984. Mechanics of fold-and-thrust belts and accretionary wedges: Cohesive Coulomb theory. Journal of Geophysical Research 89, 10087-10101.

Evans, D.J.A. 2000. Quaternary geology and geomorphology of the Dinosaur Provincial Park area and surrounding plains, Alberta, Canada: the identification of former glacial lobes, drainage diversions and meltwater flood tracks. Quaternary Science Reviews 19, 931–958.

Evans, D.J.A. 2007. Glacitectonic structures and landforms. Encyclopaedia of Quaternary Science, Elsevier Publishing, Oxford, 831-838.

Evans, D.J.A. In press. Till: A Glacial Process Sedimentology. Wiley Blackwell, Chichester.

Evans, D.J.A., England, J.H. 1991. Canadian landform examples 19: high Arctic thrust block moraines. Canadian Geographer. 35, 93-97.

Evans, D.J.A., Benn, D.I. 2004. Facies description and the logging of sedimentary exposures. In: Evans, D.J.A., Benn, D.I. (Eds.), A Practical Guide to the Study of Glacial Sediments. Arnold, London, pp. 11-51.

Evans, D.J.A., Hiemstra, J.F., 2005. Till deposition by glacier submarginal, incremental thickening. Earth Surface Processes and Landforms 30, 1633-1662.

Evans, D.J.A., Phillips, E.R., Hiemstra, J.F., Auton, C.A. 2006. Subglacial till: formation, sedimentary characteristics and classification. Earth Science Reviews 78, 115-176.

Evans, D.J.A., Clark, C.D., Rea, B.R., 2008. Landform and sediment imprints of fast glacier flow in the southwest Laurentide Ice Sheet. Journal of Quaternary Science 23, 249–272.

Evans, D.J.A., Hiemstra, J.F., Ó Cofaigh, C., 2007. An assessment of clast macrofabrics in glaciogenic sediments based on A/B plane data. Geografiska Annaler A89, 103-120.

Evans, D.J.A., Young, N.J., Cofaigh, C., 2014. Glacial geomorphology of terrestrial terminating fast flow lobes/ice stream margins in the southwest Laurentide ice sheet. Geomorphology 204, 86–113.

Evans, D.J.A., Storrar, R.D., Rea, B.R. 2016. Crevasse-squeeze ridge corridors: Diagnostic features of late-stage palaeo-ice stream activity. Geomorphology 258, 40-50.

Evans, D.J.A., Atkinson, N., Phillips, E.R. In prep. Glacial geomorphology of the Neutral Hills Uplands, Alberta, Canada: on the process-form imprints of dynamic ice streams and ice lobes. Geomorphology.

Eyles, N., Eyles, C.H., Miall, A.D. 1983. Lithofacies types and vertical profile models; an alternative approach to the description and environmental interpretation of glacial diamict and diamictite sequences. Sedimentology 30, 393-410.

Fenton, M.M., Langenberg, W., Pawlowicz, J. 1993. Glacial deformation phenomena of east-central Alberta in the Stettler-Coronation region. Field trip B-1, Guidebook. Geological Association of Canada, Mineralogical Association of Canada, pp 46.

Fenton, M.M., Waters, E.J., Pawley, S.M., Atkinson, N., Utting, D.J., Mckay, K. 2013. Surficial geology of Alberta. Alberta Geological Survey, AER/AGS Map 601.

Gehrmann, A., Hüneke, H., Meschede, M., Phillips, E. 2016. 3D microstructural architecture of deformed glacigenic sediments associated with large-scale glacitectonism, Jasmund Peninsula (NE Rügen), Germany. Journal of Quaternary Science DOI: 10.1002/jqs.2843.

Glombick P. 2010. Top of the Belly River Group in the Alberta Plains: subsurface stratigraphic picks and modelled surface. Energy Resources Conservation Board, ERCB/AGS Open File 2010-10, pp 27.

Gravenor, C.P., Kupsch, W.O. 1959. Ice disintegration features in western Canada. Journal of Geology 67, 48–64.

Harris, C., Brabham, P., Williams, G.D. 1995. Glaciotectonic structures and their relation to topography at Dinas Dinlle, Arvon, northwest Wales. Journal of Quaternary Science 10, 397–399.

Harris, C., Williams, G., Brabham, P., Eaton, G., McCarroll, D. 1997. Glaciotectonized Quaternary sediments as Dinas Dinlle, Gwynedd, North Wales, and the bearing on the style of deglaciation in the eastern Irish Sea. Quaternary Science Reviews 16, 109-127.

Hiemstra, J.F., Evans, D.J.A., Ó Cofaigh, C. 2007. The role of glaciotectonic rafting and comminution in the production of subglacial tills: examples from SW Ireland and Antarctica. Boreas 36, 386–399.

Hicock, S.R., Goff, J.R., Lian, O.B., Little, E.C. 1996. On the interpretation of subglacial till fabric. Journal of Sedimentary Research 66, 928–934.

Hopkins, O.B., 1923. Some structural features of the plains area of Alberta caused by Pleistocene glaciation. Bulletin of the Geological Society of America 34, 419–430.

Hooyer, T.S., Iverson, N.R. 2000. Diffusive mixing between shearing granular layers: constraints on bed deformation from till contacts. Journal of Glaciology 46, 641–651.

Huuse, M., Lykke-Andersen, H. 2000. Overdeepened Quaternary valleys in the eastern Danish North Sea: morphology and origin. Quaternary Science Reviews 19, 1233-1253.

Ildefonse, B., Mancktelow, N.S. 1993. Deformation around rigid particles: the influence of slip at the particle/matrix interface. Tectonophysics 221, 345–359.

Johnson, M.D., Clayton, L. 2003. Supraglacial landsystems in lowland terrain. In: Evans, D.J.A. (Ed.), Glacial Landsystems. Arnold, London, 228–251.

Kjær, K.H., Larsen, E., van der Meer, J.J.M., Ingólfsson, Ó., Krüger, J., Benediktsson, Í.Ö., Knudsen, C.G., Schomacker, A. 2006. Subglacial decoupling at the sediment/bedrock interface: a new mechanism for rapid flowing ice. Quaternary Science Reviews 25, 2704-2712.

Kupsch, W.O. 1962. Ice-thrust ridges in western Canada. Journal of Geology 70, 582–594.

Lee, J.R., Phillips, E., Booth, S.J., Rose, J., Jordan, H.M., Pawley, S.M., Warren, M., Lawley, R.S. 2013. A polyphase glacitectonic model for ice-marginal retreat and terminal moraine development: the Middle Pleistocene British Ice Sheet, northern Norfolk, UK. Proceedings of the Geologists Association, 124. 753-777.

Lee, J.R., Phillips, E., Rose, J., Vaughan-Hirsch, D. 2016. The Middle Pleistocene glacial evolution of northern East Anglia, UK: a dynamic tectonostratigraphic–parasequence approach. Journal of Quaternary Science DOI: 10.1002/jqs.2838.

March, A. 1932. MathematischeTheorie der Regelung nach der Korngestalt bei affiner Deformation. Zeitschrift fur Kristallographie 81, 285-297.

Moran, S.R., Clayton, L., Hooke, R., Fenton, M.M., Andriashek, L.D. 1980. Glacier-bed landforms of the prairie region of North America. Journal of Glaciology 25, 457-473.

Mossop, G.D., Shetsen I. 1994. Geological Atlas of the Western Canada Sedimentary Basin. Canadian Society of Petroleum Geologists and Alberta Research Council, Special Report, 510 p.

Mulugeta, G., Koyi, H. 1987. Three-dimensional geometry and kinematics of experimental piggyback thrusting. Geology 15, 1052–1056.

Nieuwland, D.A., Leutscher, J.H., Gast, J., 2000. Wedge equilibrium in fold-and thrust belts: prediction of out-of-sequence thrusting based on sandbox experiments and natural examples. Geologie en Mijnbouw/Netherlands Journal of Geosciences 79, 81–91.

Ó Cofaigh, C., Evans, D.J.A., Smith, I.R. 2010. Large-scale reorganization and sedimentation of terrestrial ice streams during late Wisconsinan Laurentide ice sheet deglaciation. Geological Society of America Bulletin, 122: 743–756.

Pedersen, S.A.S. 1987. Comparative studies of gravity tectonics in Quaternary sediments and sedimentary rocks related to fold belts. In: Jones, M.E., Preston, R.M.F. (Eds.), Sediment Deformation Mechanisms. Geological Society of London, Special Publication 29, pp. 43–65.

Pedersen, S.A.S., 1989. Glaciotectonite: brecciated sediments and cataclastic sedimentary rocks formed subglacially. In: Goldthwait, R.P., Matsch, C.L. (Eds.), Genetic Classification of Glacigenic Deposits. Balkema, Rotterdam, pp. 89–91.

Pedersen, S.A.S. 2005. Structural analysis of the Rubjerg Knude Glaciotectonic Complex, Vendsyssel, northern Denmark. Geological Survey of Denmark and Greenland Bulletin 8, 192 pp.

Pedersen, S.A.S. 2014. Architecture of Glaciotectonic Complexes. Geosciences 2014, 4, 269-296.

Pedersen, S.A.S., Boldreel, L.O. 2016. Glaciotectonic deformations in the Jammerbugt and the glaciodynamic development in the eastern North Sea. Journal of Quaternary Science (in press).

Pettapiece, W.W. 1986. Physiographic subdivisions of Alberta. Agriculture and Agri-Food Canada, Ottawa, Ontario.

Phillips, E., Merritt, J. 2008. Evidence for multiphase water-escape during rafting of shelly marine sediments at Clava, Inverness-shire, NE Scotland. Quaternary Science Reviews 27, 988-1011.

Phillips, E., Lee, J.R., Burke, H. 2008. Progressive proglacial to subglacial deformation and syntectonic sedimentation at the margins of the Mid-Pleistocene British Ice Sheet: evidence from north Norfolk, UK. Quaternary Science Reviews 27, 1848-1871.

Phillips, E., Everest, J., Reeves, H. 2012. Micromorphological evidence for subglacial multiphase sedimentation and deformation during overpressurized fluid flow associated with hydrofracturing. Boreas, 42, 395–427.

Prior, G.J., Hathway, B., Glombick, P.M., Pană, D.I., Banks, C.J., Hay, D.C., Schneider, C.L., Grobe, M., Elgr, R., Weiss, J.A. 2013. Bedrock geology of Alberta. Alberta Energy Regulator, AER/AGS Map 600, scale 1:1 000 000.

Rijsdijk, K.F., McCarroll, D., Owen, G., van der Meer, J.J.M., Warren, W.P. 1999. Clastic dykes in glacigenic diamicts: Evidence for subglacial hydrofracturing from Killiney Bay, Ireland. Sedimentary Geology 129, 111-126.

Roberts, D.H., Dackombe, R.V., Thomas, G.S.P. 2006. Palaeo-ice streaming in the central sector of the British-Irish Ice Sheet during the Last Glacial Maximum: evidence from the northern Irish Sea Basin. Boreas 36, 115-129.

Ross, M., Campbell, J.E., Parent, M., Adams, R.S. 2009. Palaeo-ice streams and the subglacial landscape mosaic of the North American mid-continental prairies. Boreas 38, 421–439.

Rotnicki, K., 1976. The theoretical basis for and a model of glaciotectonic deformation. Quaestiones Geographicae 3, 103–139.

Ruszczynska-Szenajch, H. 1987. The origin of glacial rafts: Detachment, transport, deposition. Boreas 16, 101-112.

Ruszczynska-Szenajch, H. 1988. Glaciotectonics and its relationship to other glaciogenic processes. In Croot, D.G. (ed.): Glaciotectonic Forms and Processes, 191–193. Balkema, Rotterdam.

Sauer, E.K. 1978. The engineering significance of glacier ice thrusting. Canadian Geotechnical Journal 15, 457–472.

Shetsen, I. 1987. Quaternary geology, southern Alberta. Alberta Geological Survey, Map 207.

Shetsen, I. 1990. Quaternary geology, central Alberta. Alberta Geological Survey, Map 213.

Slater, G. 1927. Structure of the Mud Buttes and Tit Hills in Alberta. Bulletin of the Geological Society of America 38.

Slater, G. 1931. The structure of the Bride Moraine, Isle of Man. Proceedings of the Liverpool Geological Society 14, 186-196.

Steinich, G. 1972. Endogene Tektonik in den Unter-Maastricht-Vorkommen auf Jasmund (Rügen). In: Geologie 20, Beiheft 71/72, S. 1 - 207. Berlin.

Thomas, G.S.P., Chiverrell, R.C. 2007. Structural and depositional evidence for repeated ice-marginal oscillation along the eastern margin of the Late Devensian Irish Sea Ice Stream. Quaternary Science Reviews 26, 2375-2405.

Thomas, G.S.P., Chiverrell, R.C. 2011. Styles of structural deformation and syntectonic sedimentation around the margins of the Late Devensian Irish Sea Ice Stream: the Isle of Man, Llyn Peninsula and County Wexford. In Phillips, E., Lee, J.R., Evans, H.M. (Eds.). 2011. Glacitectonics – Field Guide. Quaternary Research Association.

Thomas, G.S.P., Chiverrell, R.C., Huddart, D., Long, D., Roberts, D.H. 2006. The Ice Age In: Chiverrell RC and Thomas GSP (eds.). A New History of the Isle of Man: Volume 1 Evolution of the natural landscape. Liverpool University Press, 126-219.

Tsui, P.C., Cruden, D.M., Thomson, S. 1989. Ice thrust terrains and glaciotectonic settings in central Alberta. Canadian Journal of Earth Sciences 26, 1308-1318.

van Gijssel, K. 1987. A lithostratigraphic and glaciotectonic reconstruction of the Lamstedt Moraine, Lower Saxony (FRG). In: J.J.M. van der Meer (ed.). Tills and Glaciotectonics. Balkema, Rotterdam, 145-155.

van der Meer, J.J.M., Kjær, K.H., Krüger, J., Rabassa, J., Kilfeather, A.A., 2009. Under pressure: clastic dykes in glacial settings. Quaternary Science Reviews. 28, 708-720.

van der Wateren, F.M. 1985. A model of glacial tectonics, applied to the ice-pushed ridges in the central Netherlands. Bulletin of the Geological Society of Denmark 34, 55-77.

van der Wateren, F.M. 1987. Structural geology and sedimentology of the Dammer Berge push moraine, FRG. In: J.J.M. van der Meer (ed.). Tills and Glaciotectonics. Balkema, Rotterdam, 157-182.

van der Wateren, F.M. 1995. Structural geology and sedimentology of push moraines. Mededelingen Rijks Geologische Dienst 54. PhD, University of Amsterdam.

van der Wateren, F.M. 2005. Ice-marginal terrestrial landsystems: Southern Scandinavian Ice Sheet Margin. In: Evans, D.J.A. (Ed.), Glacial Landsystems. Hodder Arnold, London, pp. 166–203.

Vaughan-Hirsch, D., Phillips, E., 2016. Mid-Pleistocene thin-skinned glaciotectonic thrusting of the Aberdeen Ground Formation, Central Graben region, central North Sea. Journal of Quaternary Science (in press)

Vaughan-Hirsch, D.P., Phillips, E.R., Lee, J.R., Burke, H.F. Hart, J.K. 2011: Glacitectonic rafting of chalk bedrock: Overstrand. In Phillips, E., Lee, J. R. & Evans, H. M. (eds.): Glacitectonics – Field Guide. Quaternary Research Association, Pontypool. 198–217.

Vaughan-Hirsch, D.P., Phillips, E., Lee, J.R., Hart, J.K. 2013. Micromorphological analysis of poly-phase deformation associated with the transport and emplacement of glaciotectonic rafts at West Runton, north Norfolk, UK. Boreas 42, 376–394.

Williams, G., Brabham, P., Eaton, G., Harris, C., 2001. Late Devensian glaciotectonic deformation at St Bees, Cumbria: a critical wedge model. Journal of the Geological Society 158, 125–135.

## 11. Figures

**Figure 1. (a)** DEM showing place names referred to in text and major geomorphological features of the study area and its regional context. Inset shows the surficial geology of the study area (from Fenton *et al*., 2013. E: aeolian deposits; LG: glaciolacustrine deposits; FG: glaciofluvial deposits; M: undifferentiated moraine (diamict); MS: stagnation moraine; MF: fluted moraine; MT: ice thrust moraine); and **(b)** Features identified on the DEM include major glacitectonic thrust masses (green shade) and the margins and flow directions (circled numbers and arrows) of the main ice flow phases including, from oldest to youngest, 1 (white), 2 (pink), 3 (blue), 4 (black), 5 (red) and 6 (yellow). Major moraines (from Evans *et al*., in prep) include: HM – Handel Moraine of Evans *et al.* (2016); AM – Altario Moraine; VM – Veteran Moraine; GIM – Grassy Island Moraine; MB – Mud Buttes.

**Figure 2.** Annotated DEM of the field area, showing major moraines and other major glacial landforms (from Evans *et al*., in prep). Also outlined are areas of major glacitectonically thrust masses (green outline), significant hummocky terrain (blue outline) and fluted thrust moraine (black outline).

**Figure 3.** Annotated DEM of the Misty Hills and associated landforms. The Misty Hills thrust structures are outlined in pink and the direction of ice flow related to their original

construction is designated by the pre-2 ice flow phase arrows. Subsequent ice lobe margins and flow phases are identified by blue lines and arrows (phase 3a and 3b) and black arrows for phase 4, during which the Mud Buttes and a further cupola hill to the north were constructed and overrun.

**Figure 4. (a)** Annotated aerial image (Google Earth) of the Mud Buttes, SW Monitor, Alberta, Canada; **(b)** Structural geology map of the Mud Buttes thrust complex (inset showing the location of the Mud Buttes); **(c)** to **(g)** Lower hemisphere stereographic projections showing the structural data - **(c)** and **(d)** bedding (dip and dip-direction), **(e)** and **(f)** thrusts/faults (dip and dip-direction), **(g)** folds (plunge); and **(h)** Rose diagram showing trend of fold axes.

**Figure 5.** Large-scale thrusting and repetition of Belly River Group sandstones, siltstones and mudstones within structural domain 1 of the Mud Buttes thrust complex [UTM 0531208 5743775]. **(a)** and **(c)** photographs of the large-scale deformation structures developed within the Belly River Group; **(b)** and **(d)** interpretive line drawings of the exposed sections.

**Figure 6. (a)** Large-scale thrusting and repetition of Belly River Group sandstones, siltstones and mudstones within structural domain 1 of the Mud Buttes thrust complex; **(b)** and **(c)** Asymmetrical, inclined asymmetrical anticline-syncline fold pair (see Figure 3a for location of fold) [UTM 0530927 5743980]; **(d)** Detail of asymmetrical S-C fabric developed within thrust indicating a southerly directed sense of shear on this structure [UTM 0530927 5743980].

**Figure 7.** Large-scale thrusting and repetition of Belly River Group sandstones, siltstones and mudstones within structural domain 2a of the Mud Buttes thrust complex: **(a)** and **(b)** Large-scale synclines developed within the foot-walls of two prominent northerly dipping thrusts [UTM 0531021 5744096]; and **(c)** Folding and thrusting characteristic of structural domain 2a [UTM 0531294 5743835].

**Figure 8. (a)** to **(c)** Large-scale thrusting and repetition of Belly River Group sandstones, siltstones and mudstones within structural domain 2a of the Mud Buttes thrust complex. Note the progressive increase in the angle of dip of the thrust slices from south to north across the domain [(a) UTM 0531285 5743922; (b) UTM 0531399 5743894; (c) UTM 0531320 5743983].

**Figure 9. (a)** and **(b)** Large-scale, upright ‘box-like’ anticline deforming not only bedding within the Belly River Group but also a set of earlier developed low-angle (relative to bedding) to bedding-parallel (T1) thrusts [UTM 0530992 5744093]; **(c)** Large-scale, upright, M-shaped ‘box-like’ anticline developed adjacent to the southern margin of structural domain 2a; and **(d)** Parasitic minor folds developed upon a mesoscale south-verging anticline and

syncline fold pair. Note that the folds deform a set of earlier developed (T1) thrusts and a later set of small-scale, southerly directed (T2) thrusts developed within the core of the anticline [UTM 0531385 5744105].

**Figure 10. (a)** and **(b)** Large-scale thrusting of the Belly River Group within domain 2a. The prominent thrust planes are preferentially developed within the weaker mudstones immediately adjacent to the bases of the more competent sandstones. The thrust planes are marked by thin lenses of fissile, organic-rich mudstones [UTM 0531320 5743983]; **(c)** and **(d)** Well-developed, asymmetrical S-C fabrics developed within narrow brittle-ductile shear zones cutting the Belly River Group sandstones and siltstones in structural domain 3 [(c) [UTM 0531205 5744179]; (d) UTM 0531212 5744159]; and **(e)** Large-scale, upright fold in domain 2b truncated by a gently north-dipping thrust interpreted as marking the base of structural domain 4 [UTM 0531510 5744107].

**Figure 11.** Large-scale folding and thrusting of structural domain 2b [UTM 0530992 5744174]. Note the zone of complex folding and thrusting developed within the unit of thinly interbedded sandstones, siltstones and mudstones.

**Figure 12.** Large-scale folding and thrusting within the core of the Mud Buttes thrust complex and characteristic of structural domain 2b: **(a)** and **(b)** Steeply inclined, tight to isoclinal, southerly verging folds deforming the sandstones of the Belly River Group [UTM 0531078 5744120]. Not that the very tight to isoclinal fold toward the centre of the photograph is deformed by a number of brittle thrusts; **(c)** and **(d)** Large-scale southerly verging folds deforming a 2 to 3 m thick sandstone unit within the Belly River Group [UTM 0531221 5744112].

**Figure 13. (a)** and **(b)** Photograph (a) and interpretive line drawing (b) showing the zone of intense brittle-ductile shearing which characterises structural domain 3 of the Mud Buttes thrust complex [UTM 0531212 5744159]; **(c)** Truncated, non-cylindrical, isoclinal folds deforming the sandstones within the shear zone marking the southern boundary of structural domain 3 [UTM 0531385 5744105]; and **(d)** Intense ductile shearing within a more mudstone-rich unit exposed adjacent to the southern margin of structural domain 3 [UTM 0531385 5744105].

**Figure 14.** Large-scale folding and thrusting characterising structural domain 4 located on the northern side of the Mud Buttes thrust complex [(a) and (b) UTM 0531267 5744288; (c) and (d) UTM 0531178 5744379].

**Figure 15.** Previously published structural cross-sections through the Mud Buttes thrust complex: **(a)** Slater (1927) (fig. 1 of Slater, 1927); and **(b)** Fenton *et al*. (1993) (fig. 16 of Fenton *et al*., 1993).

**Figure 16.** Lithological log and field photograph of the section through the Quaternary sediments overlying the glacitectonised bedrock exposed in section MBQ 1.

**Figure 17. (a)** to **(c)** Photographs showing the vertical continuum of well-exposed, deformed and sheared mudstone capped by a poorly exposed, clay-rich diamicton exposed within section MBQ 2.

**Figure 18.** Lithological photolog **(a)** and sedimentological details **(b)** of the section through the Quaternary sediments overlying the glacitectonised bedrock exposed in section MBQ 3. Details in (b) show: i) deformed sandstone intraclasts and boudins; ii) rotten sandstone clasts arranged in discrete horizontal lines and lying directly above the striated bedrock surface; iii) striations on the bedrock surface with rose plot of striation alignments.

**Figure 19.** Lithological log and field photograph of the section through the Quaternary sediments overlying the glacitectonised bedrock exposed in section MBQ 4. Also shown is spherical Gaussian weighted, contoured lower hemisphere stereographic projection of the clast macrofabric data obtained from the diamicton exposed the top of this sequence.

**Figure 20. (a)** Ternary diagram of $I = S_3/S_1$ versus $E = 1-(S_2/S_1)$ for the clast macrofabrics at sections MBQ 4 and MBQ 5. Also shown are the fields defined by clasts macrofabrics from the glacitectonite continuum (Evans *et al*., 1988), subglacial till (Evans and Hiemstra, 2005) and lodged clasts (Evans and Hiemstra, 2005); and **(b)** Graph showing the variation in clast macrofabric modality versus $S_3/S_1$ isotropy.

**Figure 21.** Lithological log and field photograph of the section through the Quaternary sediments overlying the glacitectonised bedrock exposed in section MBQ 5. Also shown is spherical Gaussian weighted, contoured lower hemisphere stereographic projection of the clast macrofabric data obtained from the diamicton exposed at this locality.

**Figure 22.** Composite vertical logs with genetic facies codes for the Quaternary stratigraphic sequences exposed at Mud Buttes.

**Figure 23.** Schematic cross-section through the Mud Buttes showing the structural architecture of this glacitectonic thrust complex (see text for details) (see Figure 1b for the approximate location of the line of section).

**Figure 24. (a)** to **(h)** Cartoon showing the evolution of the Mud Buttes thrust complex as a result of proglacial deformation and this landform being subsequently overridden by ice during a later readvance to form a dome-like cupola hill (see text for details).

# 12. Tables

**Table 1.** Pollen types detected in the organic-rich clayey-silt exposed at Section MBQ 4

| **Species** | **Sample 15008/1** | **Sample 15008/2 upper** | **Sample 15008/2 lower** |
|---|---|---|---|
| Pine | 1 | | |
| Hazel | 1 | | |
| Grass | 1 | | |
| Artemisia | 2 | | 1 |
| Spruce/fir | | 1 | |
| Tsuga | | 1 | |
| Sedges | | 3 | |
| Rumex | | 1 | |
| *Scrophulariaceae* | | 2 | |
| *Chenopodiaceae* | | | 1 |

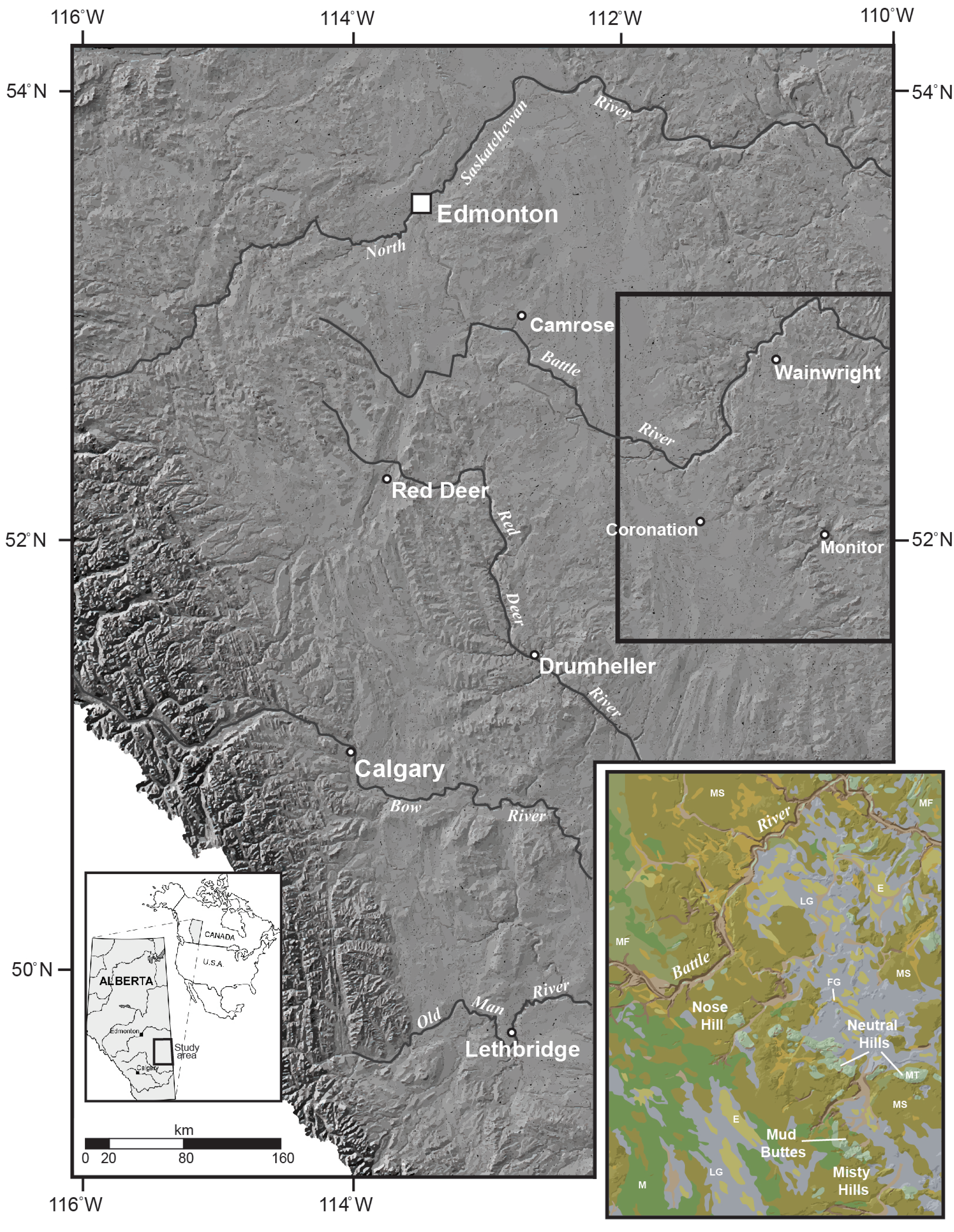
116°W
114°W
112°W
110°W
54°N
52°N
50°N
North
Saskatchewan
River
Edmonton
Camrose
Battle
River
Wainwright
Red Deer
Red
Deer
River
Coronation
Monitor
Drumheller
Calgary
Bow
River
Old
Man
River
Lethbridge
CANADA
U.S.A.
ALBERTA
Edmonton
Calgary
Study area
km
0
20
80
160
MS
MF
River
LG
E
MF
Battle
MS
FG
Nose Hill
Neutral Hills
MT
MS
E
Mud Buttes
LG
M
Misty Hills

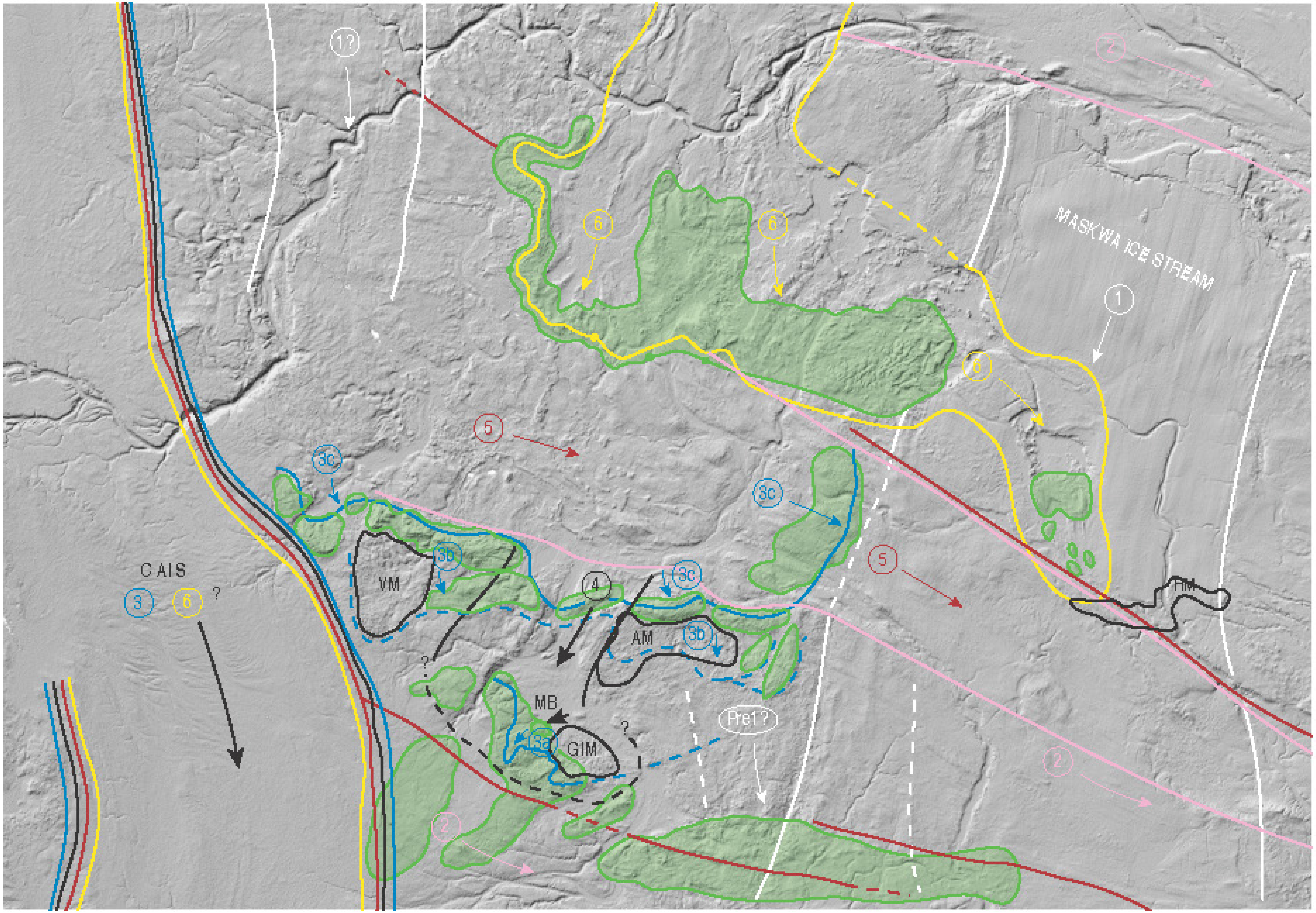

MASKWA ICE STREAM
CAIS
VM
AM
MB
GIM
HM
Pre1?
1?
1
2
3
3a
3b
3c
4
5
6

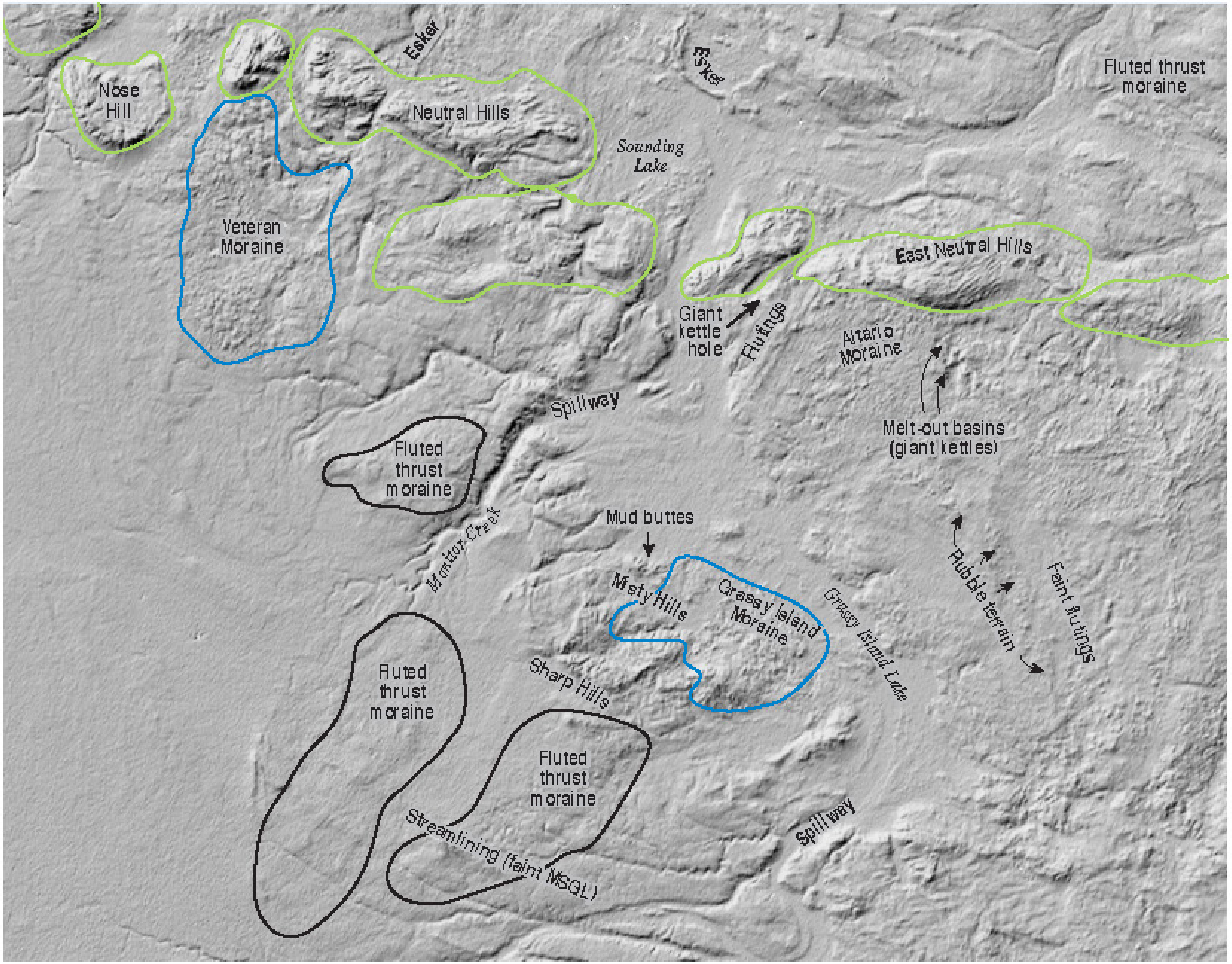
Esker
Esker
Fluted thrust moraine
Nose Hill
Neutral Hills
Sounding Lake
Veteran Moraine
East Neutral Hills
Giant kettle hole
Flutings
Altario Moraine
Spillway
Melt-out basins (giant kettles)
Fluted thrust moraine
Monitor Creek
Mud buttes
Misty Hills
Grassy Island Moraine
Grassy Island Lake
Rubble terrain
Faint flutings
Fluted thrust moraine
Sharp Hills
Fluted thrust moraine
Streamlining (feint MSGL)
Spillway

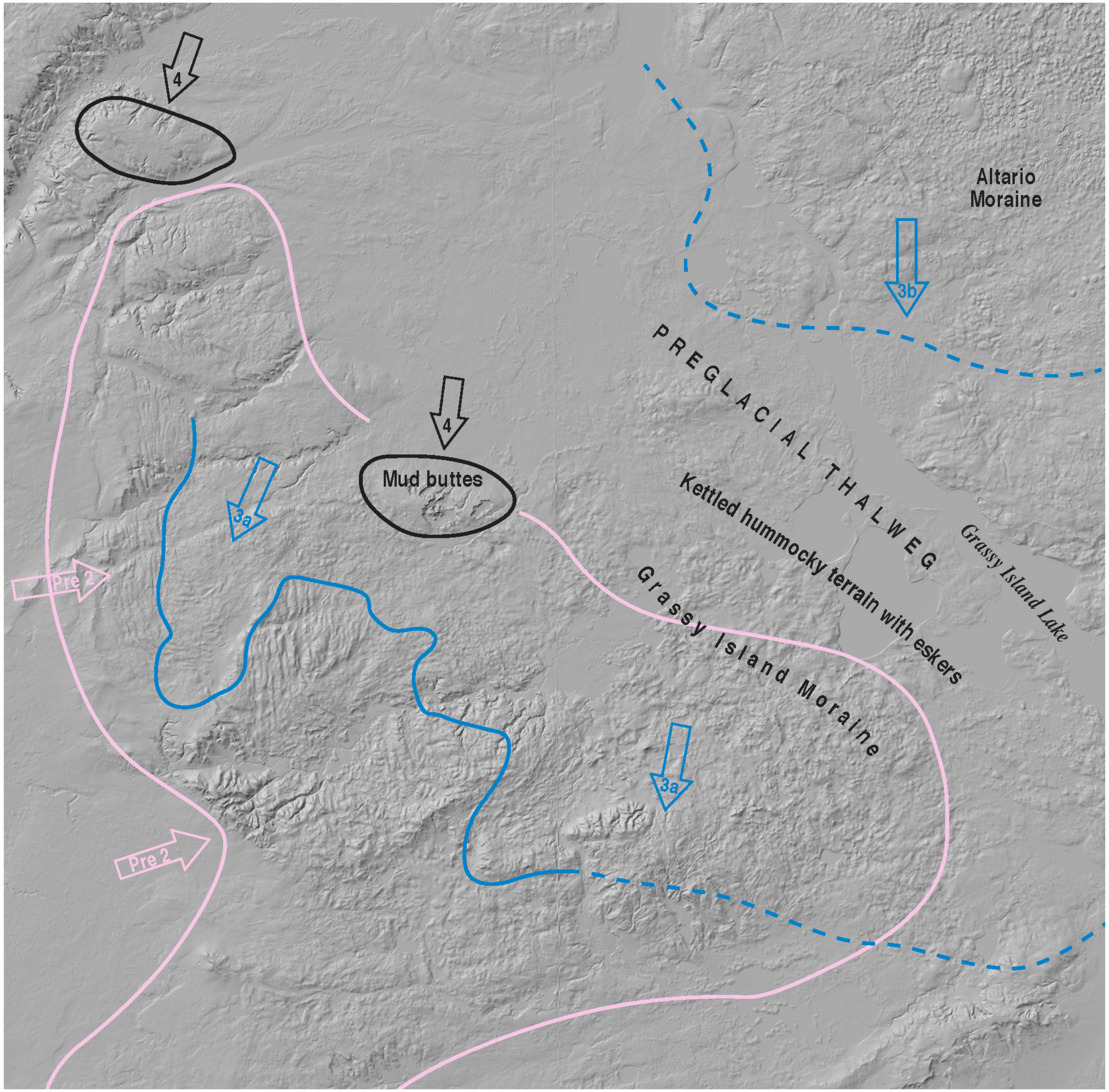

4
4
Mud buttes
3a
3a
3b
Pre 2
Pre 2
Altario Moraine
PREGLACIAL THALWEG
Kettled hummocky terrain with eskers
Grassy Island Moraine
Grassy Island Lake

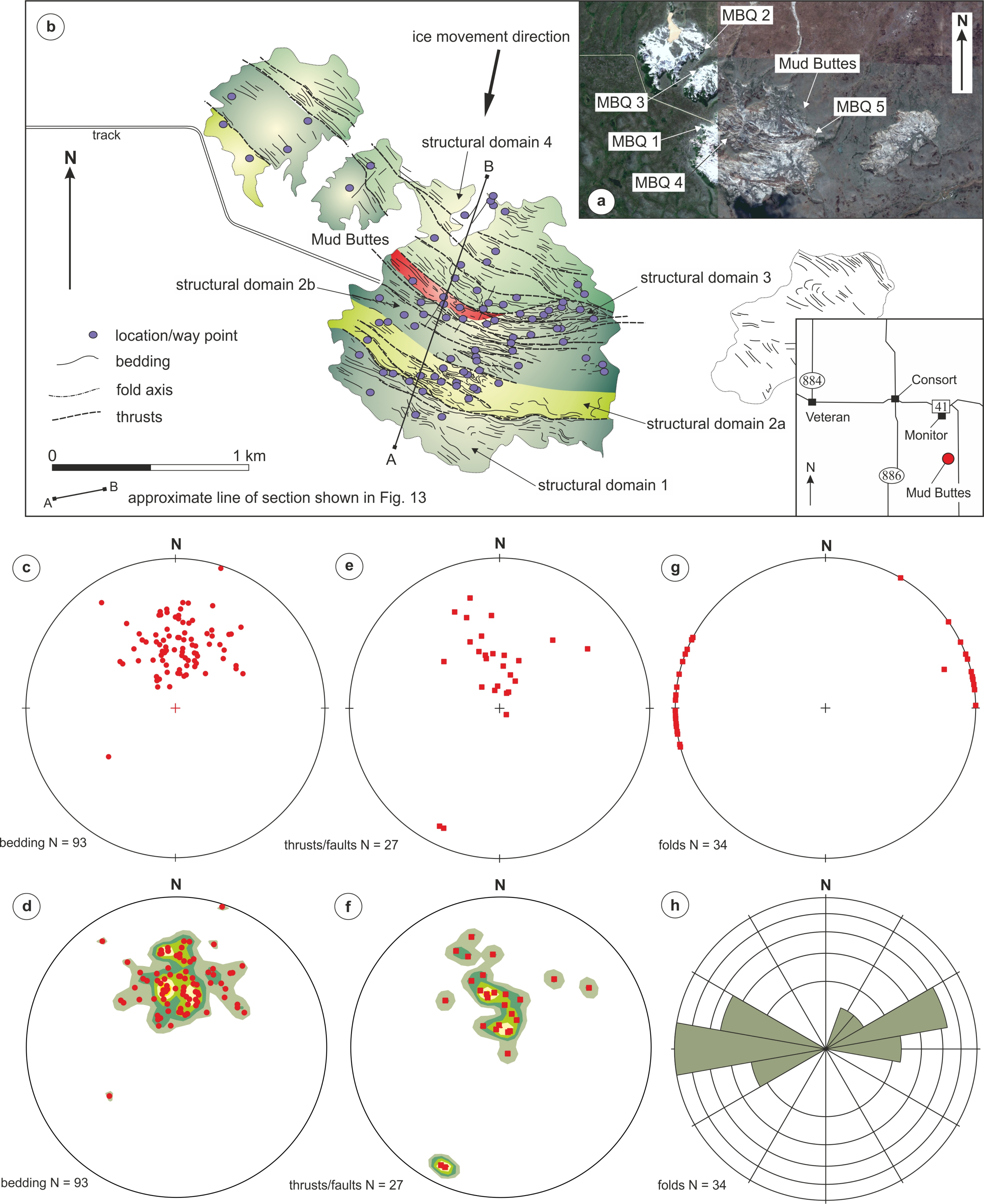

b
ice movement direction
track
N
structural domain 4
B
Mud Buttes
structural domain 2b
structural domain 3
location/way point
bedding
fold axis
thrusts
structural domain 2a
0
1 km
A
structural domain 1
A
B
approximate line of section shown in Fig. 13
MBQ 2
MBQ 3
Mud Buttes
MBQ 5
MBQ 1
MBQ 4
a
N
884
Consort
41
Veteran
Monitor
N
886
Mud Buttes
c
N
bedding N = 93
e
N
thrusts/faults N = 27
g
N
folds N = 34
d
N
bedding N = 93
f
N
thrusts/faults N = 27
h
N
folds N = 34

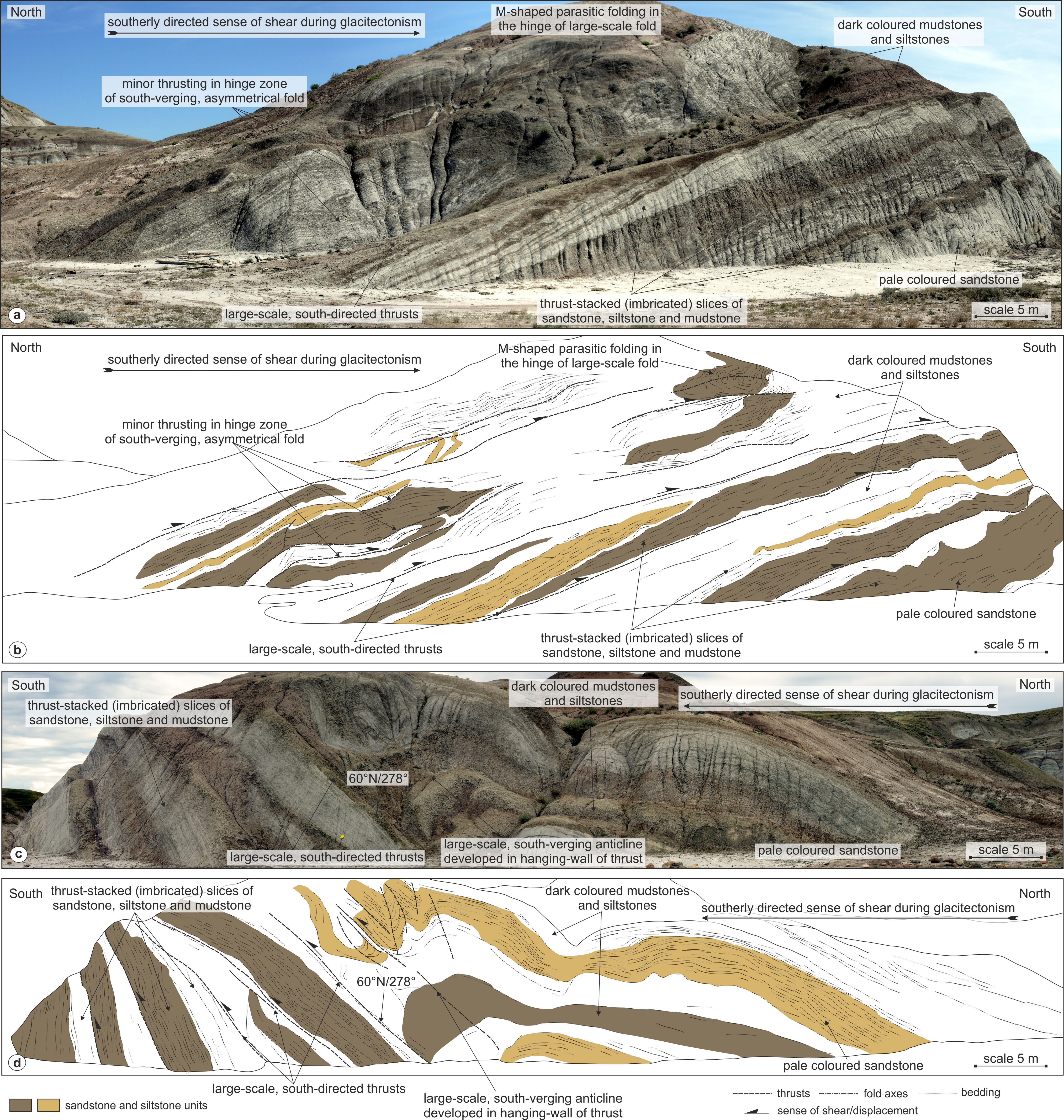
North
South
southerly directed sense of shear during glacitectonism
M-shaped parasitic folding in the hinge of large-scale fold
dark coloured mudstones and siltstones
minor thrusting in hinge zone of south-verging, asymmetrical fold
pale coloured sandstone
thrust-stacked (imbricated) slices of sandstone, siltstone and mudstone
large-scale, south-directed thrusts
scale 5 m
a
North
South
southerly directed sense of shear during glacitectonism
M-shaped parasitic folding in the hinge of large-scale fold
dark coloured mudstones and siltstones
minor thrusting in hinge zone of south-verging, asymmetrical fold
pale coloured sandstone
thrust-stacked (imbricated) slices of sandstone, siltstone and mudstone
large-scale, south-directed thrusts
scale 5 m
b
South
North
dark coloured mudstones and siltstones
southerly directed sense of shear during glacitectonism
thrust-stacked (imbricated) slices of sandstone, siltstone and mudstone
60°N/278°
large-scale, south-directed thrusts
large-scale, south-verging anticline developed in hanging-wall of thrust
pale coloured sandstone
scale 5 m
c
South
thrust-stacked (imbricated) slices of sandstone, siltstone and mudstone
dark coloured mudstones and siltstones
North
southerly directed sense of shear during glacitectonism
60°N/278°
pale coloured sandstone
scale 5 m
d
large-scale, south-directed thrusts
large-scale, south-verging anticline developed in hanging-wall of thrust
sandstone and siltstone units
thrusts
fold axes
bedding
sense of shear/displacement

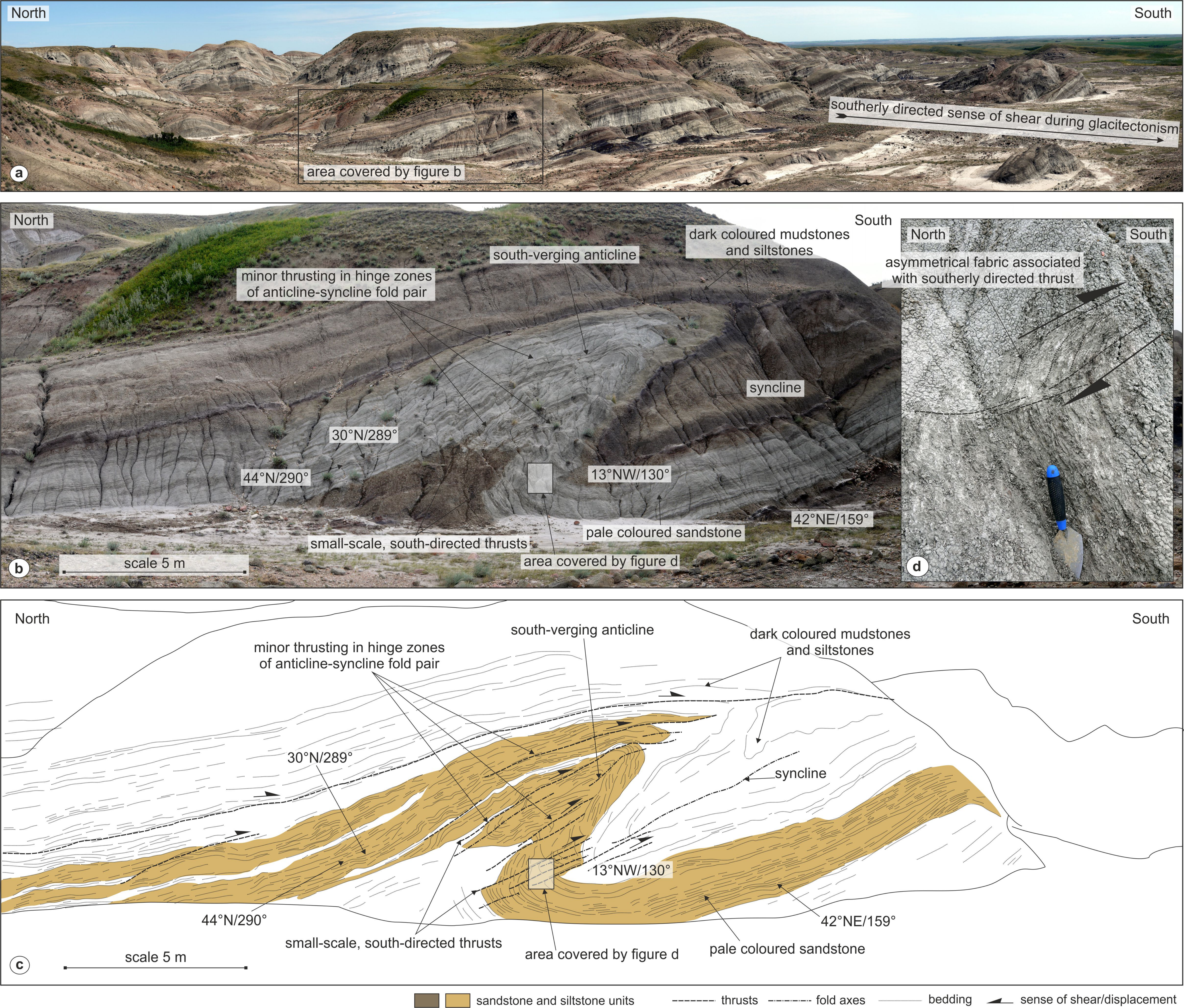

North
South
southerly directed sense of shear during glacitectonism
area covered by figure b
a
North
South
dark coloured mudstones and siltstones
south-verging anticline
minor thrusting in hinge zones of anticline-syncline fold pair
syncline
30°N/289°
44°N/290°
13°NW/130°
42°NE/159°
pale coloured sandstone
small-scale, south-directed thrusts
area covered by figure d
scale 5 m
b
North
South
asymmetrical fabric associated with southerly directed thrust
d
North
South
south-verging anticline
dark coloured mudstones and siltstones
minor thrusting in hinge zones of anticline-syncline fold pair
30°N/289°
syncline
13°NW/130°
44°N/290°
42°NE/159°
small-scale, south-directed thrusts
area covered by figure d
pale coloured sandstone
scale 5 m
c
sandstone and siltstone units
thrusts
fold axes
bedding
sense of shear/displacement

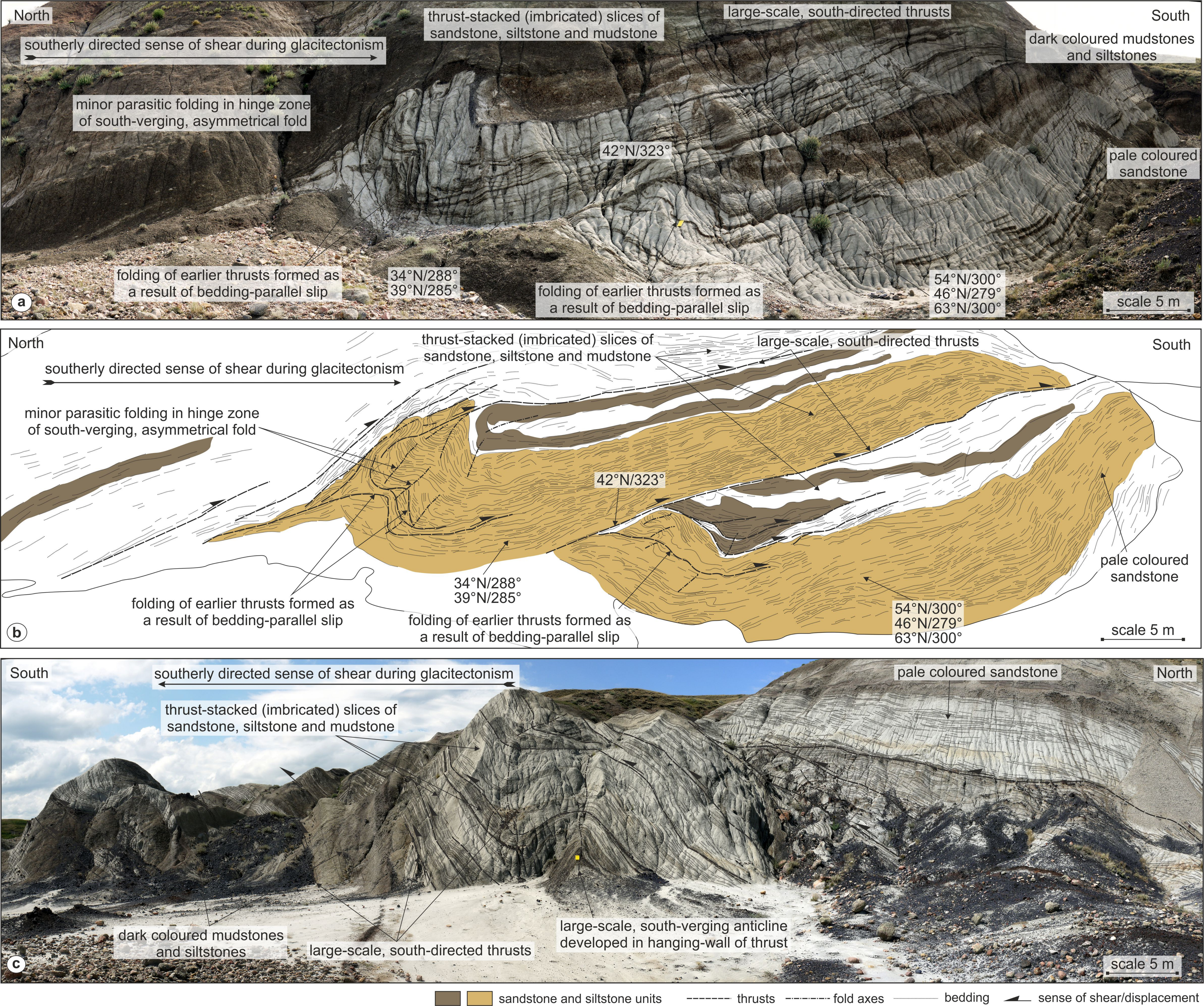
North
South
southerly directed sense of shear during glacitectonism
thrust-stacked (imbricated) slices of sandstone, siltstone and mudstone
large-scale, south-directed thrusts
dark coloured mudstones and siltstones
minor parasitic folding in hinge zone of south-verging, asymmetrical fold
42°N/323°
pale coloured sandstone
folding of earlier thrusts formed as a result of bedding-parallel slip
34°N/288°
39°N/285°
54°N/300°
46°N/279°
63°N/300°
scale 5 m
a
b
c
large-scale, south-verging anticline developed in hanging-wall of thrust
sandstone and siltstone units
thrusts
fold axes
bedding
sense of shear/displacement

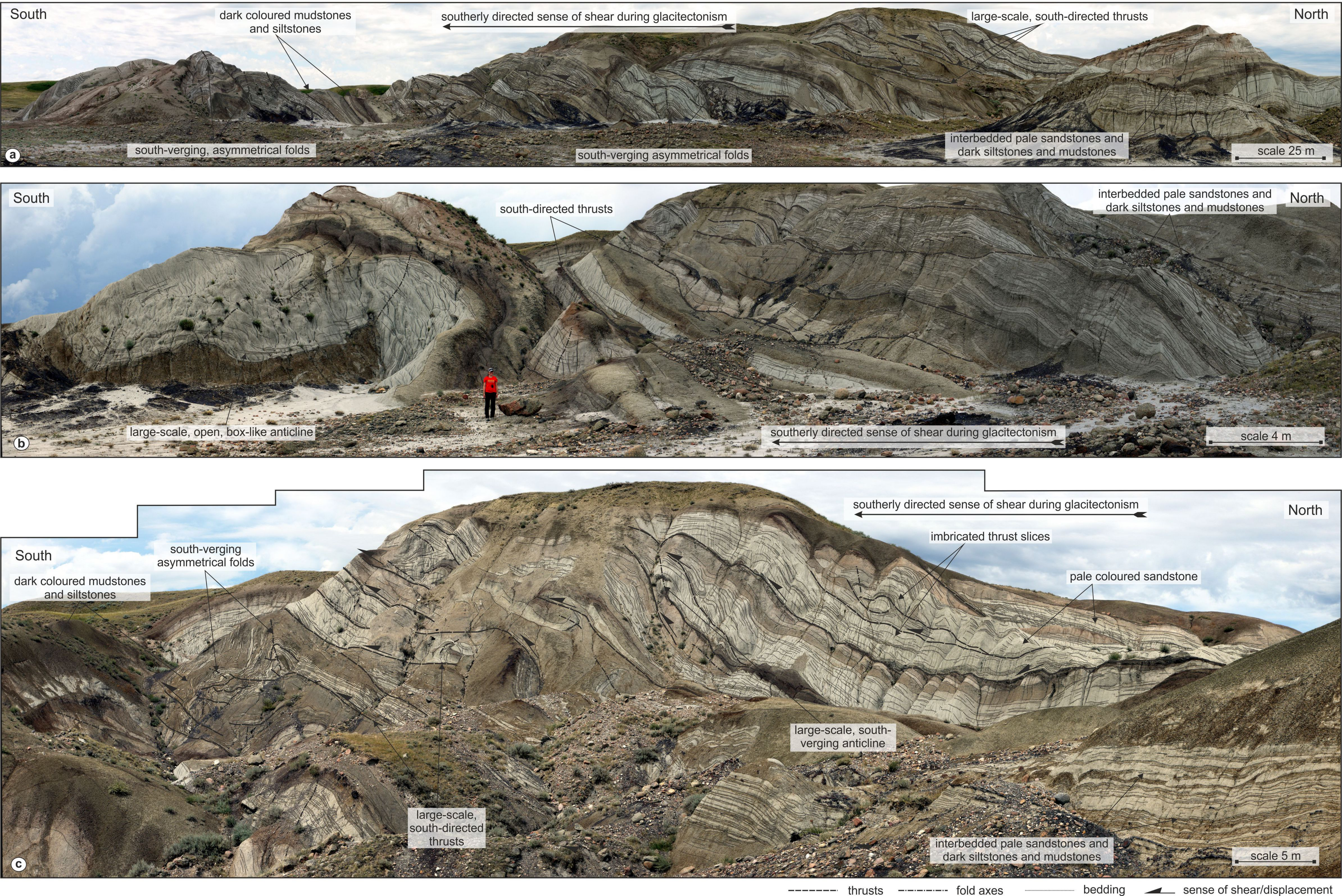
South
dark coloured mudstones and siltstones
southerly directed sense of shear during glacitectonism
large-scale, south-directed thrusts
North
south-verging, asymmetrical folds
south-verging asymmetrical folds
interbedded pale sandstones and dark siltstones and mudstones
scale 25 m
a
South
south-directed thrusts
interbedded pale sandstones and dark siltstones and mudstones
North
large-scale, open, box-like anticline
southerly directed sense of shear during glacitectonism
scale 4 m
b
southerly directed sense of shear during glacitectonism
North
South
south-verging asymmetrical folds
dark coloured mudstones and siltstones
imbricated thrust slices
pale coloured sandstone
large-scale, south-verging anticline
large-scale, south-directed thrusts
interbedded pale sandstones and dark siltstones and mudstones
scale 5 m
c
thrusts
fold axes
bedding
sense of shear/displacement

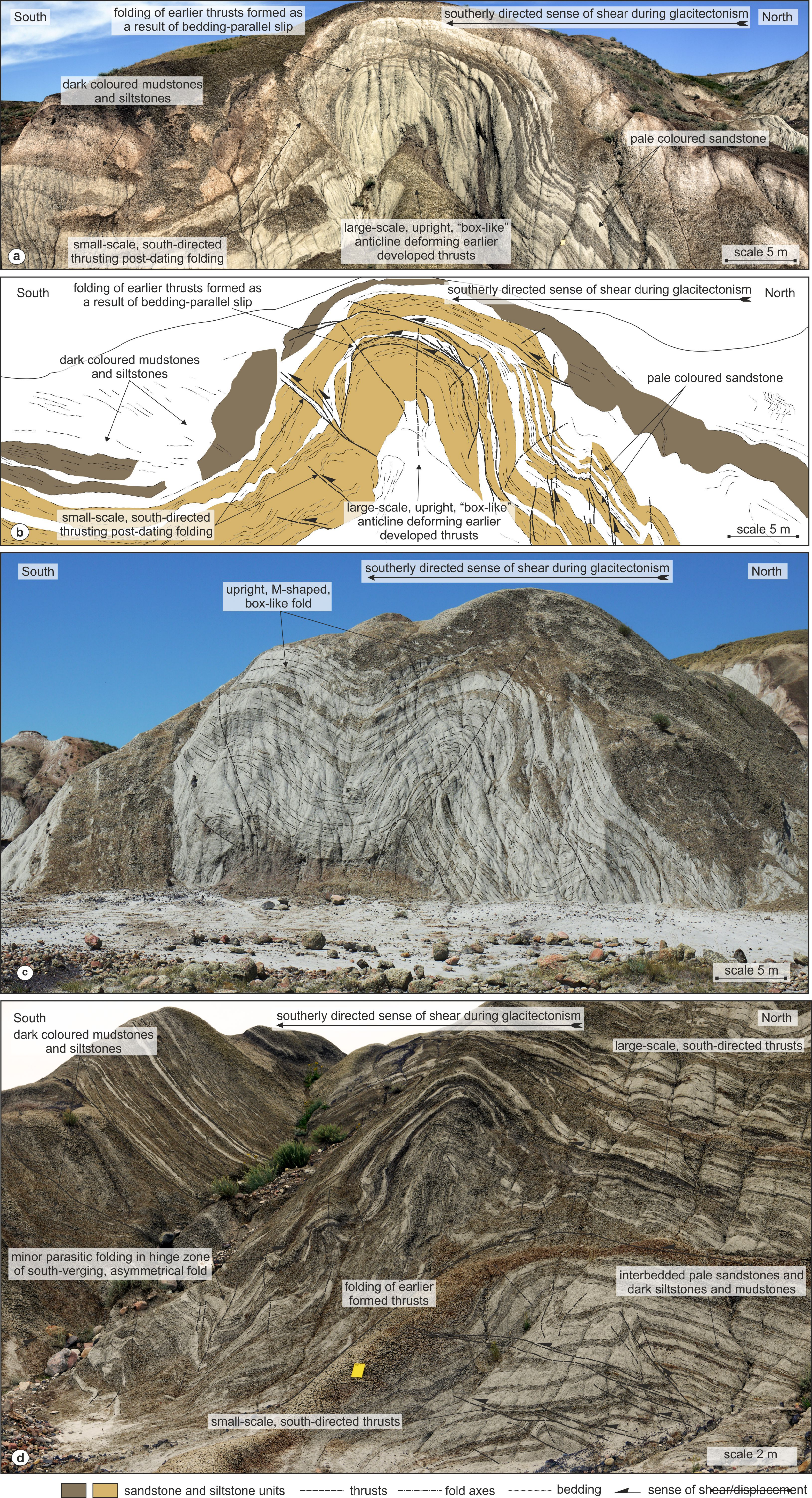
South
folding of earlier thrusts formed as a result of bedding-parallel slip
southerly directed sense of shear during glacitectonism
North
dark coloured mudstones and siltstones
pale coloured sandstone
small-scale, south-directed thrusting post-dating folding
large-scale, upright, "box-like" anticline deforming earlier developed thrusts
scale 5 m
a
South
folding of earlier thrusts formed as a result of bedding-parallel slip
southerly directed sense of shear during glacitectonism
North
dark coloured mudstones and siltstones
pale coloured sandstone
small-scale, south-directed thrusting post-dating folding
large-scale, upright, "box-like" anticline deforming earlier developed thrusts
scale 5 m
b
South
southerly directed sense of shear during glacitectonism
North
upright, M-shaped, box-like fold
scale 5 m
c
South
dark coloured mudstones and siltstones
southerly directed sense of shear during glacitectonism
North
large-scale, south-directed thrusts
minor parasitic folding in hinge zone of south-verging, asymmetrical fold
folding of earlier formed thrusts
interbedded pale sandstones and dark siltstones and mudstones
small-scale, south-directed thrusts
scale 2 m
d
sandstone and siltstone units
thrusts
fold axes
bedding
sense of shear/displacement

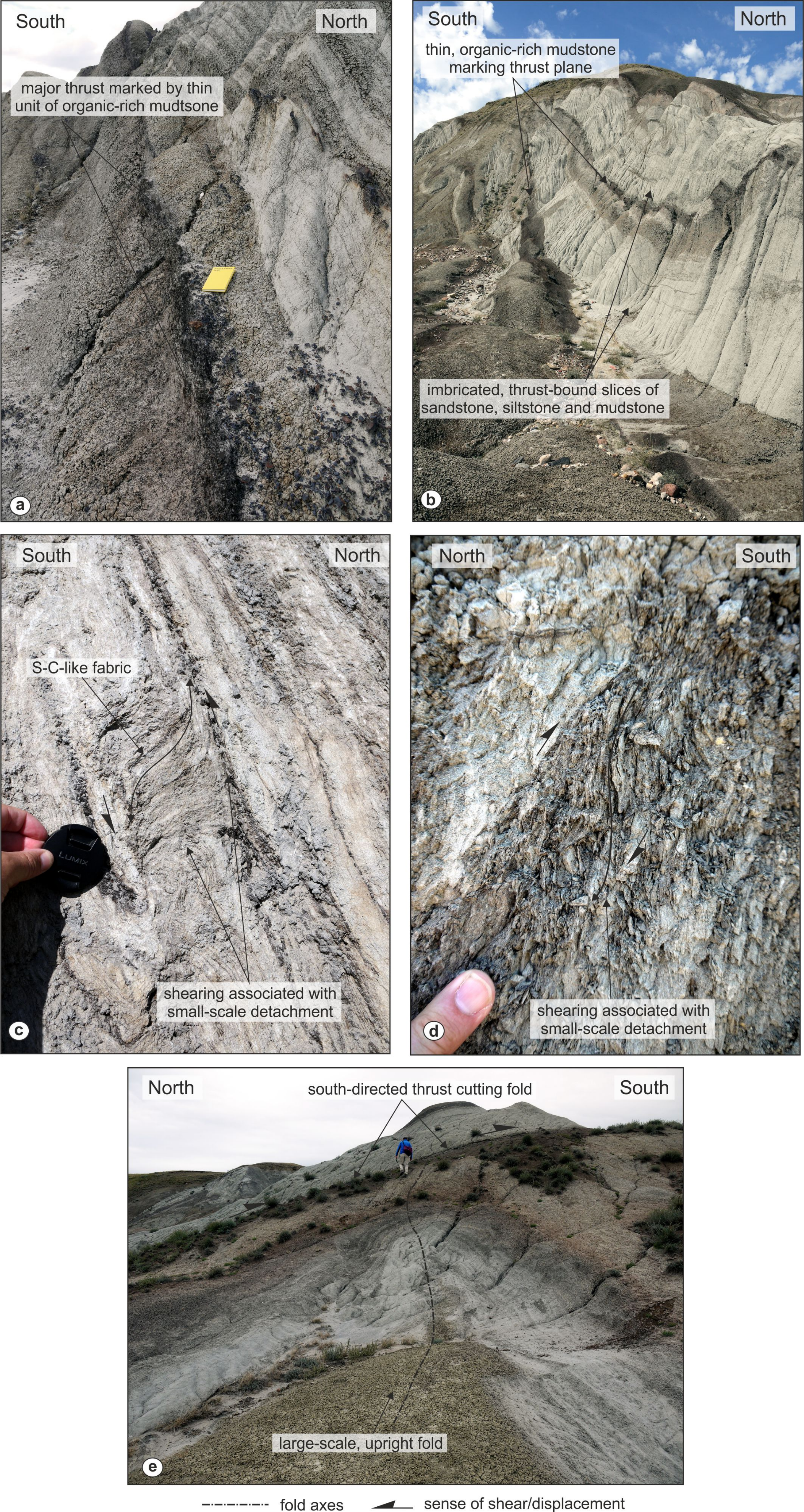
South
North
major thrust marked by thin unit of organic-rich mudtsone
a
South
North
thin, organic-rich mudstone marking thrust plane
imbricated, thrust-bound slices of sandstone, siltstone and mudstone
b
South
North
S-C-like fabric
LUMIX
shearing associated with small-scale detachment
c
North
South
shearing associated with small-scale detachment
d
North
South
south-directed thrust cutting fold
large-scale, upright fold
e
fold axes
sense of shear/displacement

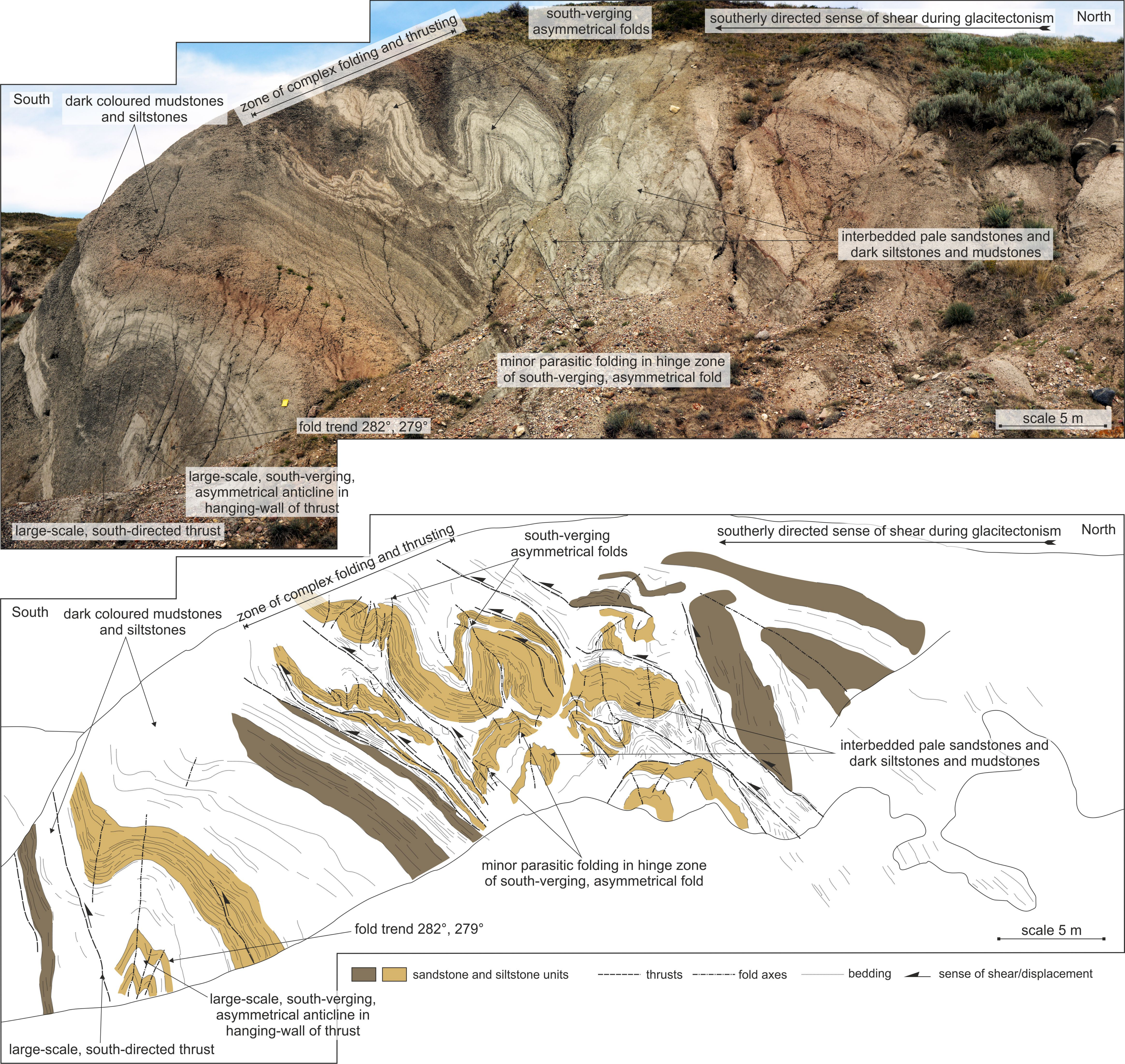
South
North
dark coloured mudstones and siltstones
zone of complex folding and thrusting
south-verging asymmetrical folds
southerly directed sense of shear during glacitectonism
interbedded pale sandstones and dark siltstones and mudstones
minor parasitic folding in hinge zone of south-verging, asymmetrical fold
fold trend 282°, 279°
large-scale, south-verging, asymmetrical anticline in hanging-wall of thrust
large-scale, south-directed thrust
scale 5 m
sandstone and siltstone units
thrusts
fold axes
bedding
sense of shear/displacement

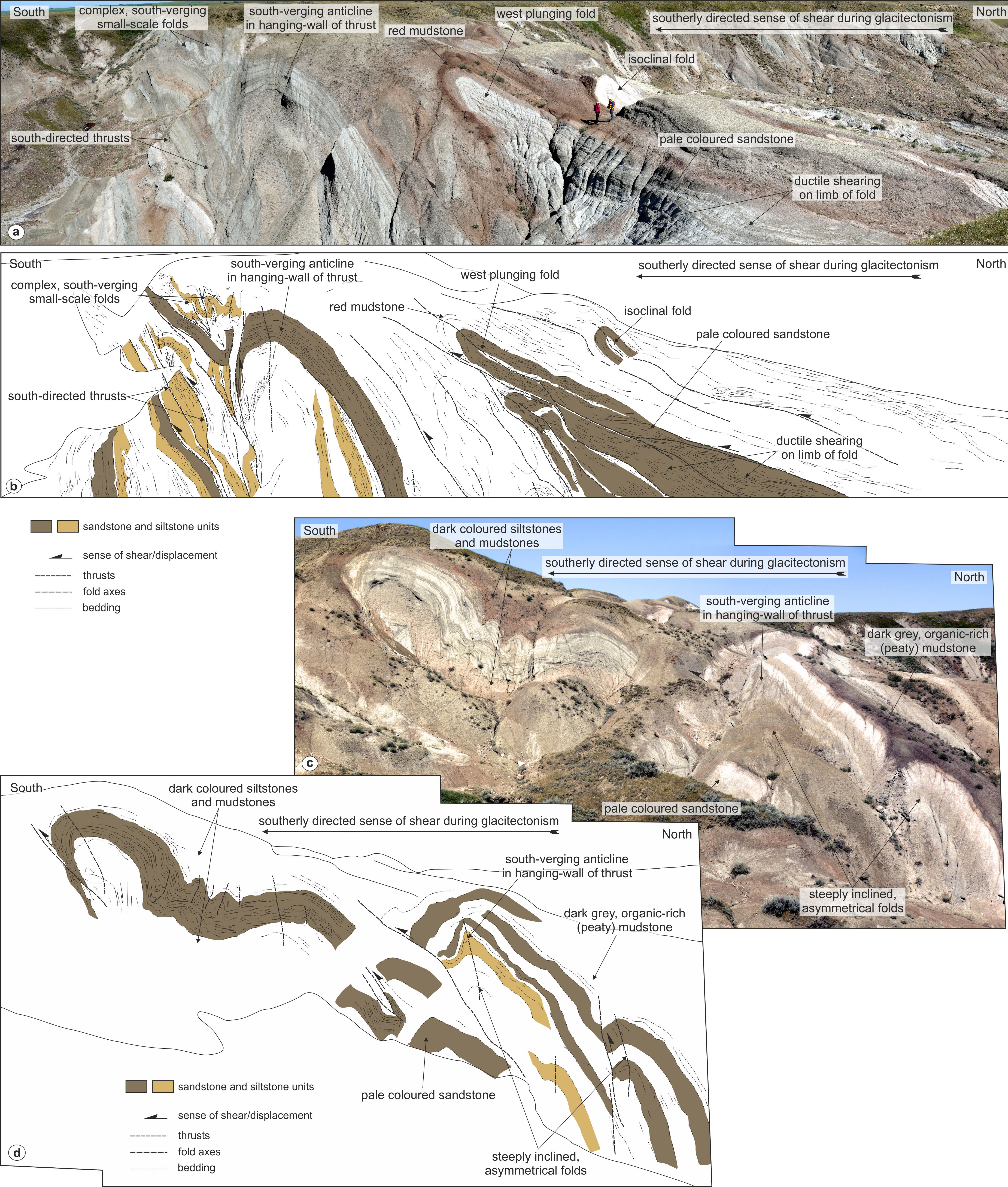
South
complex, south-verging small-scale folds
south-verging anticline in hanging-wall of thrust
red mudstone
west plunging fold
southerly directed sense of shear during glacitectonism
North
isoclinal fold
south-directed thrusts
pale coloured sandstone
ductile shearing on limb of fold
a
South
south-verging anticline in hanging-wall of thrust
southerly directed sense of shear during glacitectonism
North
complex, south-verging small-scale folds
west plunging fold
red mudstone
isoclinal fold
pale coloured sandstone
south-directed thrusts
ductile shearing on limb of fold
b
sandstone and siltstone units
sense of shear/displacement
thrusts
fold axes
bedding
South
dark coloured siltstones and mudstones
southerly directed sense of shear during glacitectonism
North
south-verging anticline in hanging-wall of thrust
dark grey, organic-rich (peaty) mudstone
pale coloured sandstone
steeply inclined, asymmetrical folds
c
South
dark coloured siltstones and mudstones
southerly directed sense of shear during glacitectonism
North
south-verging anticline in hanging-wall of thrust
dark grey, organic-rich (peaty) mudstone
sandstone and siltstone units
pale coloured sandstone
sense of shear/displacement
thrusts
fold axes
bedding
steeply inclined, asymmetrical folds
d

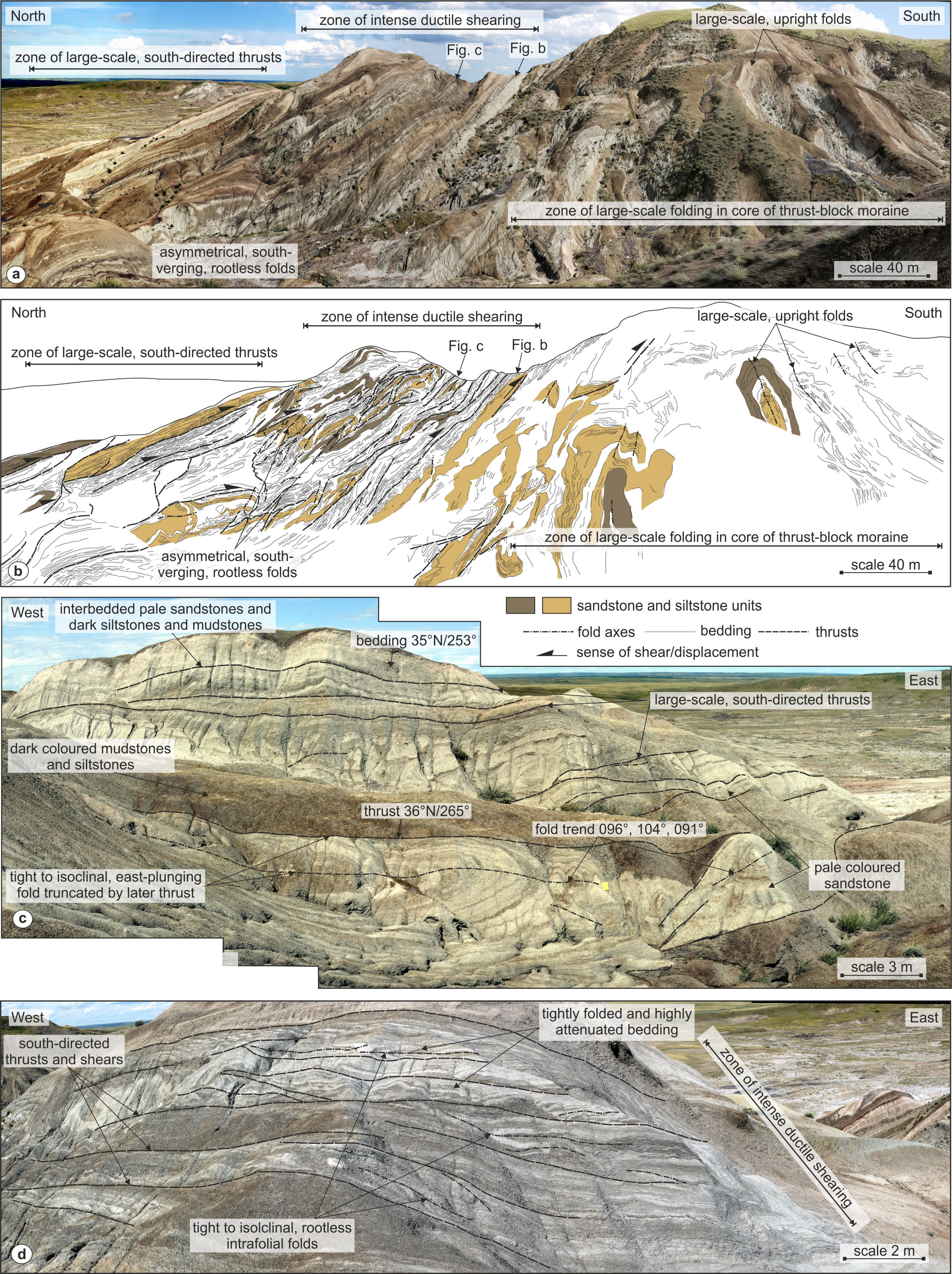
North
zone of intense ductile shearing
South
large-scale, upright folds
zone of large-scale, south-directed thrusts
Fig. c
Fig. b
zone of large-scale folding in core of thrust-block moraine
asymmetrical, south-verging, rootless folds
scale 40 m
a
North
zone of intense ductile shearing
large-scale, upright folds
South
zone of large-scale, south-directed thrusts
Fig. c
Fig. b
zone of large-scale folding in core of thrust-block moraine
asymmetrical, south-verging, rootless folds
scale 40 m
b
sandstone and siltstone units
fold axes
bedding
thrusts
sense of shear/displacement
West
interbedded pale sandstones and dark siltstones and mudstones
bedding 35°N/253°
East
large-scale, south-directed thrusts
dark coloured mudstones and siltstones
thrust 36°N/265°
fold trend 096°, 104°, 091°
tight to isoclinal, east-plunging fold truncated by later thrust
pale coloured sandstone
scale 3 m
c
West
south-directed thrusts and shears
tightly folded and highly attenuated bedding
East
zone of intense ductile shearing
tight to isolclinal, rootless intrafolial folds
scale 2 m
d

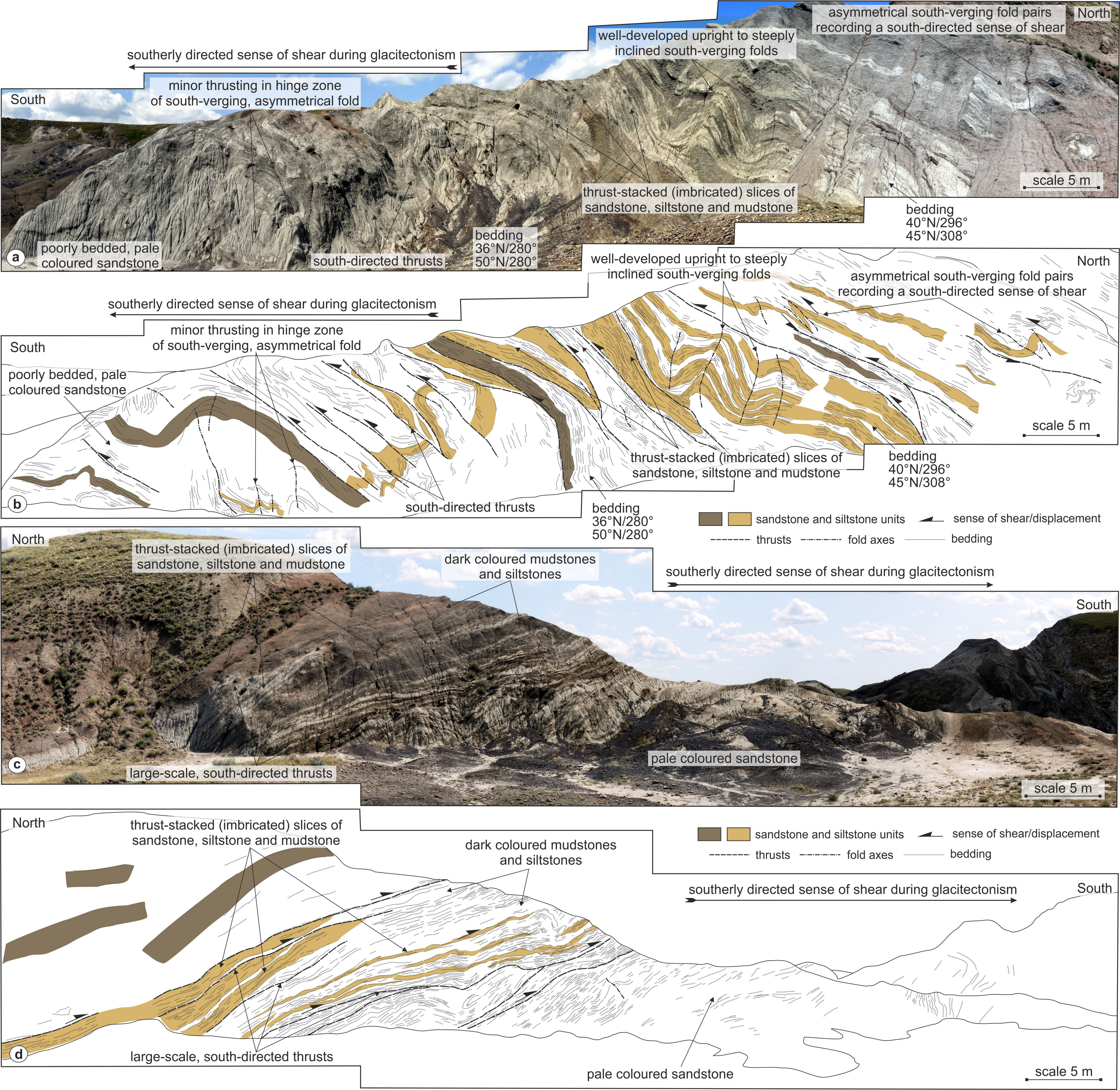

South
North
southerly directed sense of shear during glacitectonism
minor thrusting in hinge zone of south-verging, asymmetrical fold
well-developed upright to steeply inclined south-verging folds
asymmetrical south-verging fold pairs recording a south-directed sense of shear
thrust-stacked (imbricated) slices of sandstone, siltstone and mudstone
poorly bedded, pale coloured sandstone
south-directed thrusts
bedding 36°N/280° 50°N/280°
bedding 40°N/296° 45°N/308°
scale 5 m
a
b
sandstone and siltstone units
sense of shear/displacement
thrusts
fold axes
bedding
c
d
dark coloured mudstones and siltstones
large-scale, south-directed thrusts
pale coloured sandstone

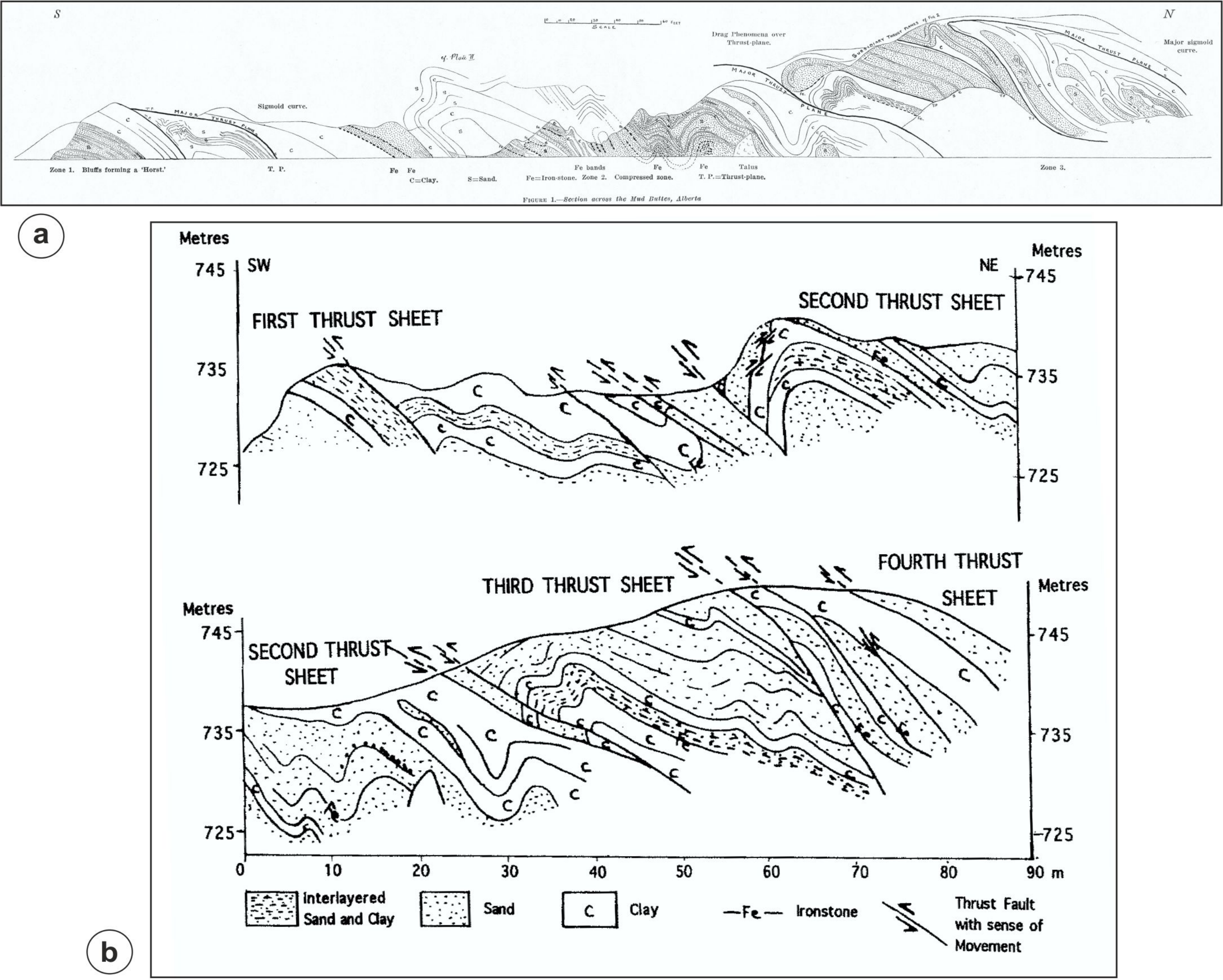

FIGURE 1.—Section across the Mud Buttes, Alberta

## Section MBQ 1

Clay-rich Dmm with indurated crumbly structure & numerous gypsum nodules

Contorted & attenuated sand & sandy, fine gravel lenses (interdigitated with overlying & underlying Dmm)

30cm

42cm

Clayey silt Dmm + numerous rotten sandstone clasts, clay intraclasts & smudged intraclasts (Type III melange)

92cm

Pale grey silty sandstone + gypsum nodules (bedrock)

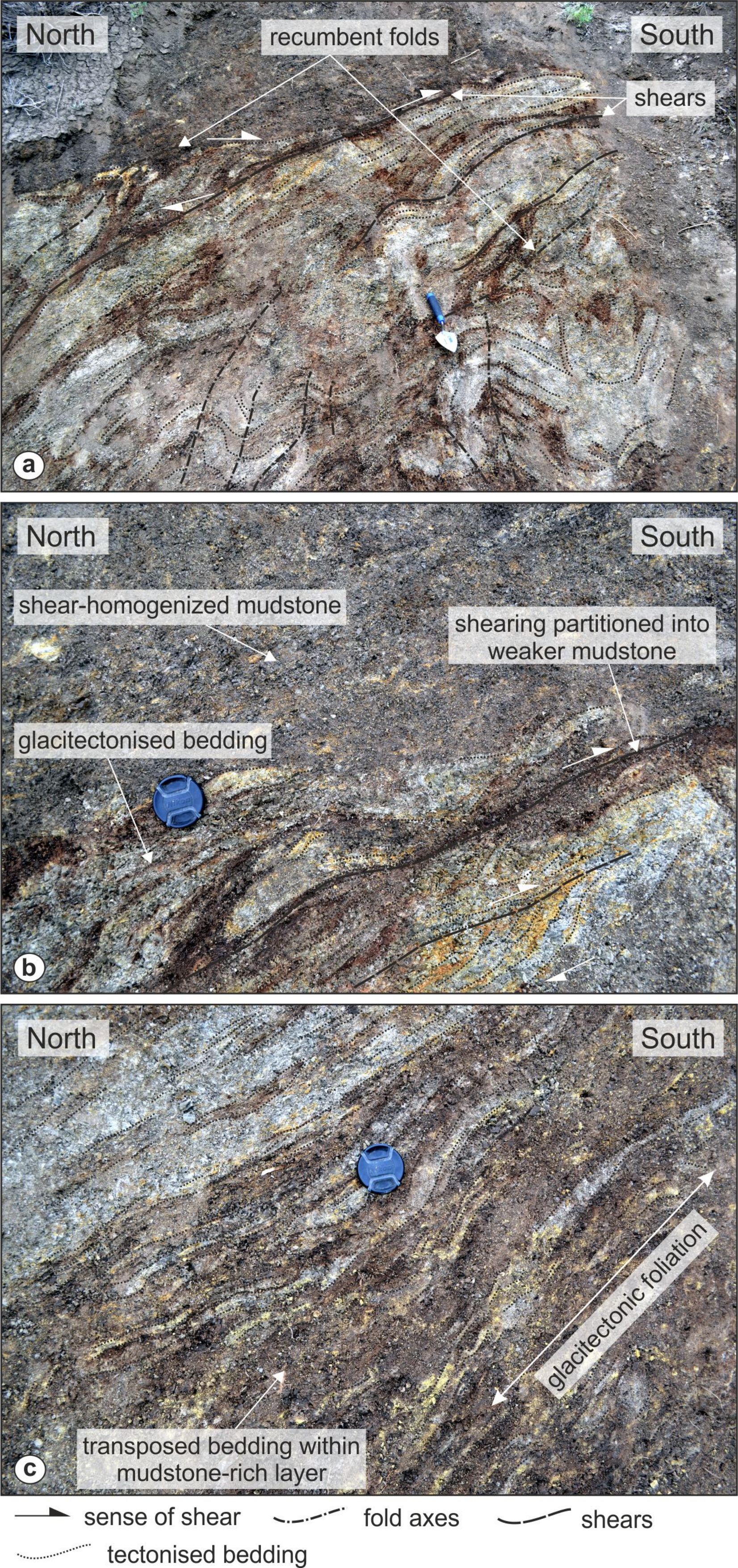
North
South
recumbent folds
shears
a
North
South
shear-homogenized mudstone
shearing partitioned into weaker mudstone
glacitectonised bedding
b
North
South
glacitectonic foliation
transposed bedding within mudstone-rich layer
c
sense of shear
fold axes
shears
tectonised bedding

# Section MBQ 3

Clay rich Dmm (massive blocky structure & gypsum nodules)

Heterogeneous diamicton (crudely bedded horizontal sands, sandy gravel, silts and clay +Dmm). Well to very highly deformed (Type III-IV melange).

0.5-1m of clayey-silt Dmm with rotten sandstone clasts (in discrete lines in basal 50cm) + sandstone boudins with deformed laminated (fine sand to silt) bedding (Type III & IV melange)

Silty sand bedrock & discontinuous boulder pavement + surface striations

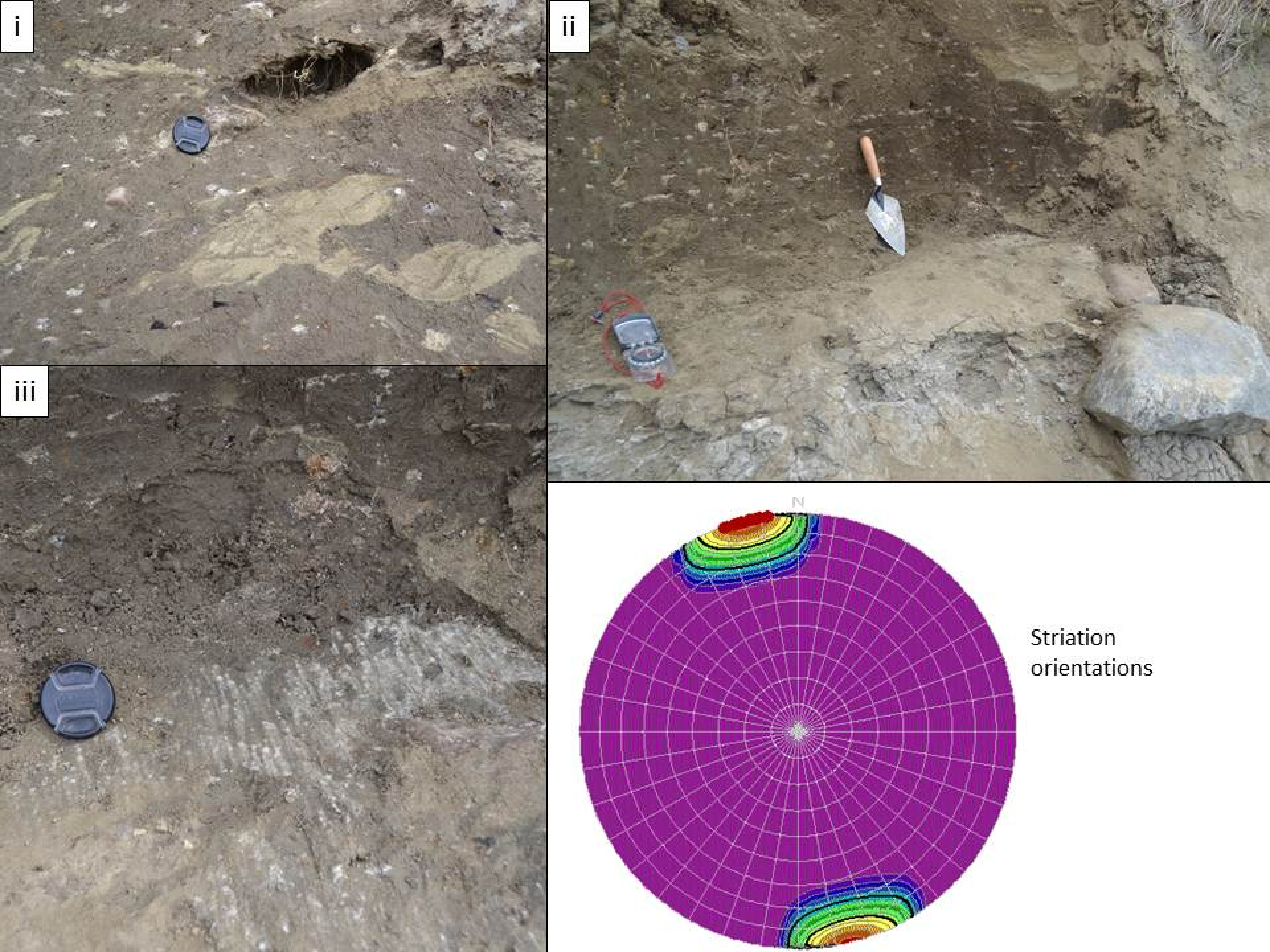
i
ii
iii
N
Striation orientations

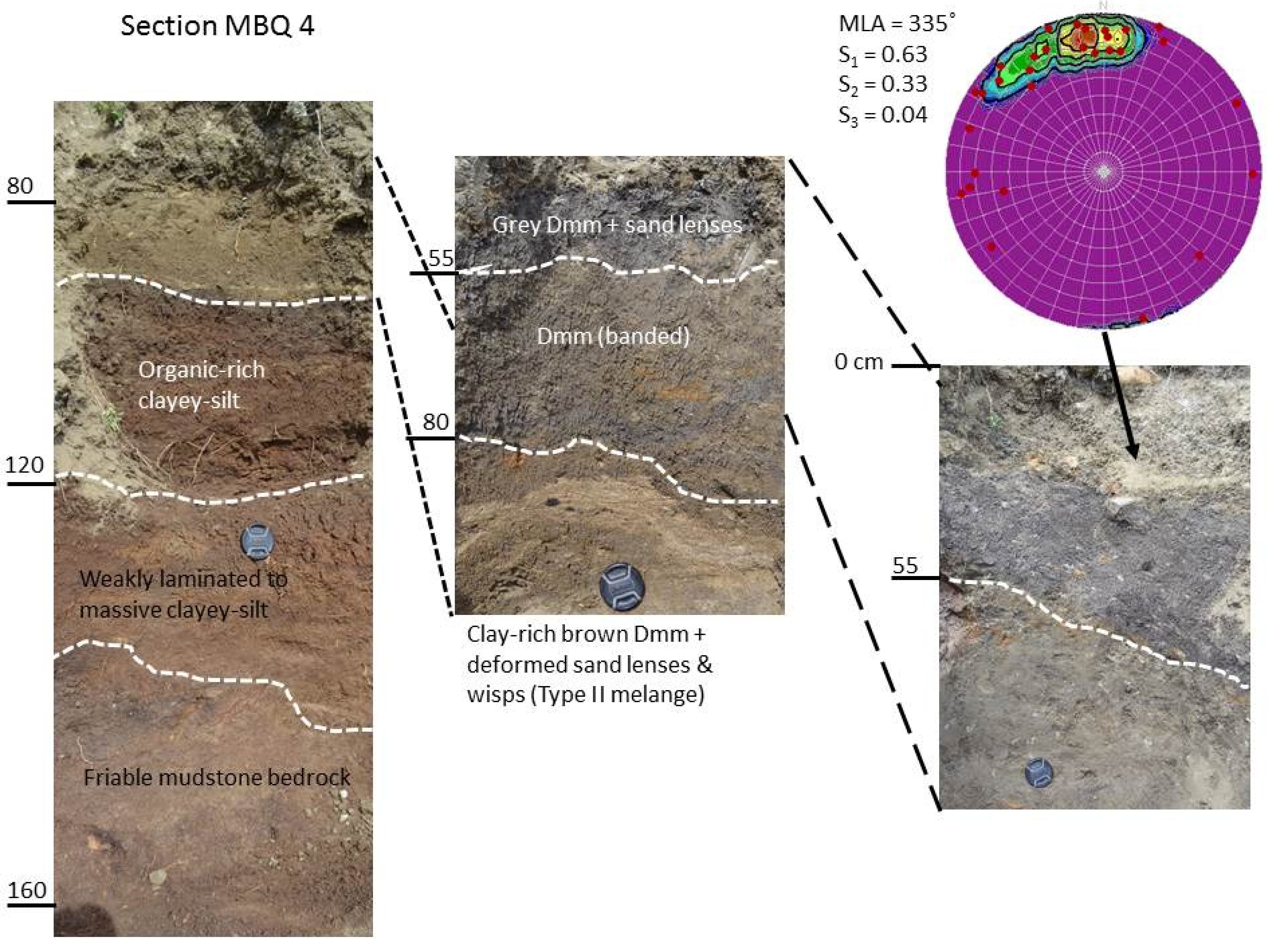

Section MBQ 4
MLA = 335°
$S_1$ = 0.63
$S_2$ = 0.33
$S_3$ = 0.04
N
80
120
160
Organic-rich clayey-silt
Weakly laminated to massive clayey-silt
Friable mudstone bedrock
55
80
Grey Dmm + sand lenses
Dmm (banded)
Clay-rich brown Dmm + deformed sand lenses & wisps (Type II melange)
0 cm
55

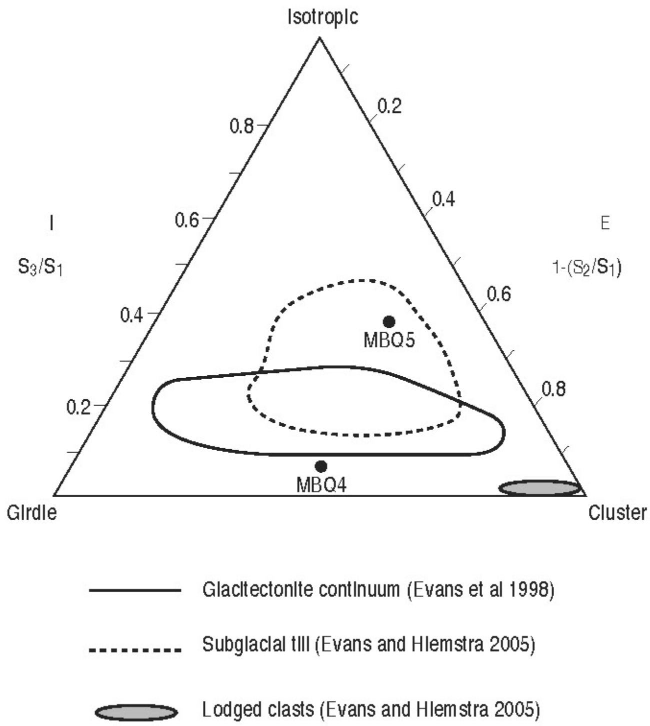
Isotropic
0.2
0.4
0.6
0.8
0.8
0.6
0.4
0.2
I
$S_3/S_1$
E
$1-(S_2/S_1)$
MBQ5
MBQ4
Girdle
Cluster
Glacitectonite continuum (Evans et al 1998)
Subglacial till (Evans and Hiemstra 2005)
Lodged clasts (Evans and Hiemstra 2005)

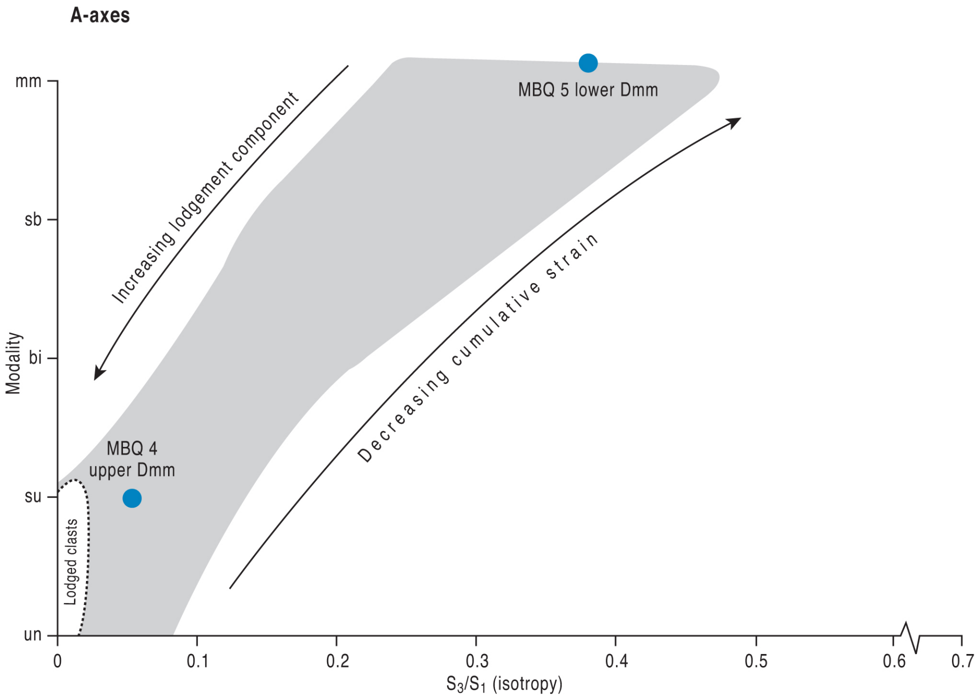

A-axes
mm
sb
bi
su
un
Modality
MBQ 5 lower Dmm
Increasing lodgement component
Decreasing cumulative strain
MBQ 4
upper Dmm
Lodged clasts
0
0.1
0.2
0.3
0.4
0.5
0.6
0.7
S3/S1 (isotropy)

Clay-rich Dmm with blocky structure (0 - 60 cm)

60 cm

Clayey silt Dmm with rotten sand clasts and lenses (boudins) occurring in discrete horizontal lines + short, discontinuous sandy stringers

MLA = 347°
$S_1$ = 0.52
$S_2$ = 0.29
$S_3$ = 0.19

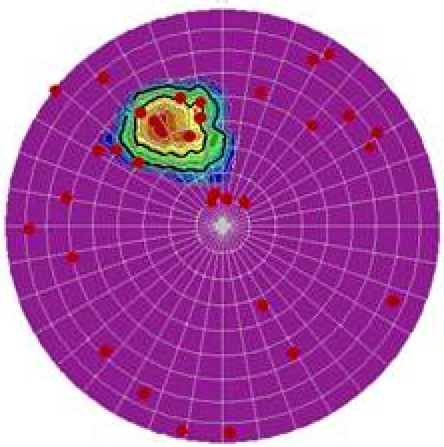

125 cm

Contorted Cretaceous strata (including folded silt, sand & clay laminae & organic units & less deformed, coherent sandstone blocks). Type III melange surrounding lodged boulders that form a clast line/pavement

145 cm

Section MBQ 5

## Figure Q7

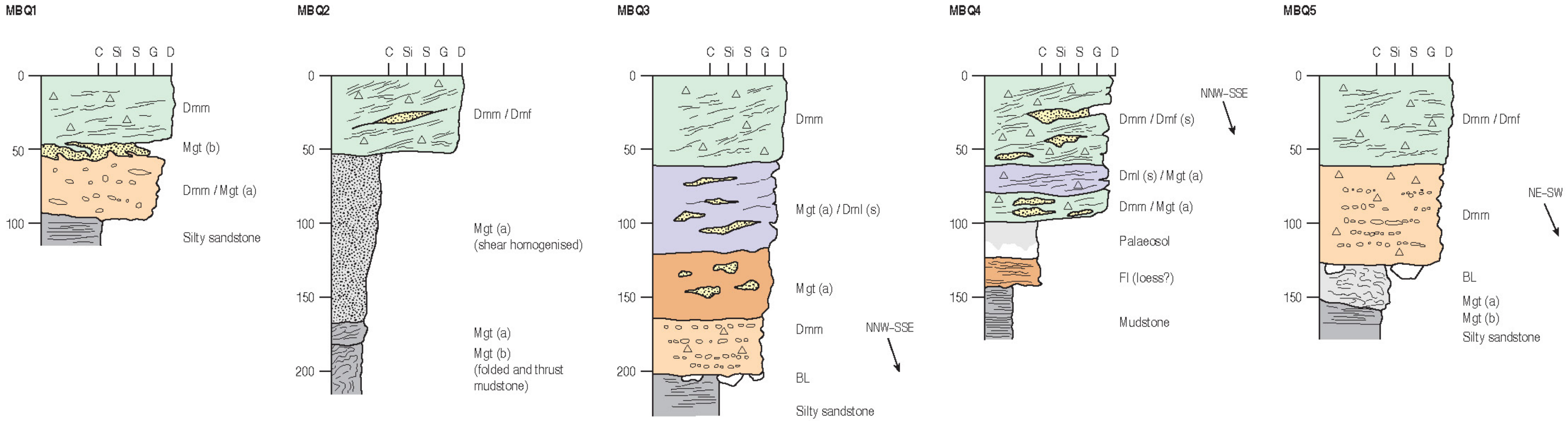
MBQ1
C Si S G D
0
50
100
Dmm
Mgt (b)
Dmm / Mgt (a)
Silty sandstone
MBQ2
C Si S G D
0
50
100
150
200
Dmm / Dmf
Mgt (a)
(shear homogenised)
Mgt (a)
Mgt (b)
(folded and thrust
mudstone)
MBQ3
C Si S G D
0
50
100
150
200
Dmm
Mgt (a) / Dml (s)
Mgt (a)
Dmm
BL
Silty sandstone
NNW–SSE
MBQ4
C Si S G D
0
50
100
150
Dmm / Dmf (s)
Dml (s) / Mgt (a)
Dmm / Mgt (a)
Palaeosol
Fl (loess?)
Mudstone
NNW–SSE
MBQ5
C Si S G D
0
50
100
150
Dmm / Dmf
Dmm
BL
Mgt (a)
Mgt (b)
Silty sandstone
NE–SW


South
North
southerly directed sense of shear during glacitectonism
bedding
thrusts
fold axes
sense of shear/displacement
sandstone and siltstone units
large-scale, south-directed thrusts
thrust-stacked (imbricated) slices of sandstone, siltstone and mudstone
south-verging, anticline-syncline fold pair
large-scale, upright, “box-like” anticline deforming earlier developed thrusts
large-scale, south-directed thrusting post-dating folding
steeply inclined south-directed thrusts
complex, south-verging folds cut by later southerly directed thrusts
steeply inclined, south-verging anticlines developed in hanging-wall of thrusts
sharp, glacitectonic boundary separating zone of large-scale folding from structurally overlying zone of intense brittle-ductile shear
zone of intense, south-directed brittle-ductile shearing
gently inclined thrusts separating zone of intense brittle-ductile shear from structurally overlying zone of folding and thrusting
thrust-stacked (imbricated) slices of sandstone, siltstone and mudstone
large-scale, south-directed thrusts
structural domain 1
structural domain 2a
structural domain 2b
structural domain 3
structural domain 4
well-developed upright to steeply inclined south-verging folds
large-scale, south-verging anticline developed in hanging-wall of thrust
minor thrusting in hinge zone of south-verging, asymmetrical fold
folding of earlier thrusts formed as a result of bedding-parallel slip
thrust-stacked (imbricated) slices of sandstone, siltstone and mudstone
folding of earlier thrusts formed as a result of bedding-parallel slip
steeply inclined, south-directed thrusts
steeply inclined, south-verging asymmetrical folds
zone of small-scale, south-verging, asymmetrical, locally rootless folds
basal thrust/décollement surface
gently to moderately dipping, south-directed thrusts
zone of gently inclined south-directed thrusts and locally developed south-verging folds
early bedding-parallel thrusts deformed by later south-verging folds
zone of intense brittle-ductile shear
upright, “box-like” folding
zone of large-scale, upright folds in core of landform
zone of gently inclined south-directed thrust and folds
south-verging folds cut by later south-directed thrusts
increasing intensity of folding and thrusting
progressively steeper inclination of bedding, thrusts and fold axial planes
progressively increase in the overall intensity of deformation
structural domain 1
structural domain 2a
structural domain 2b
structural domain 3
structural domain 4

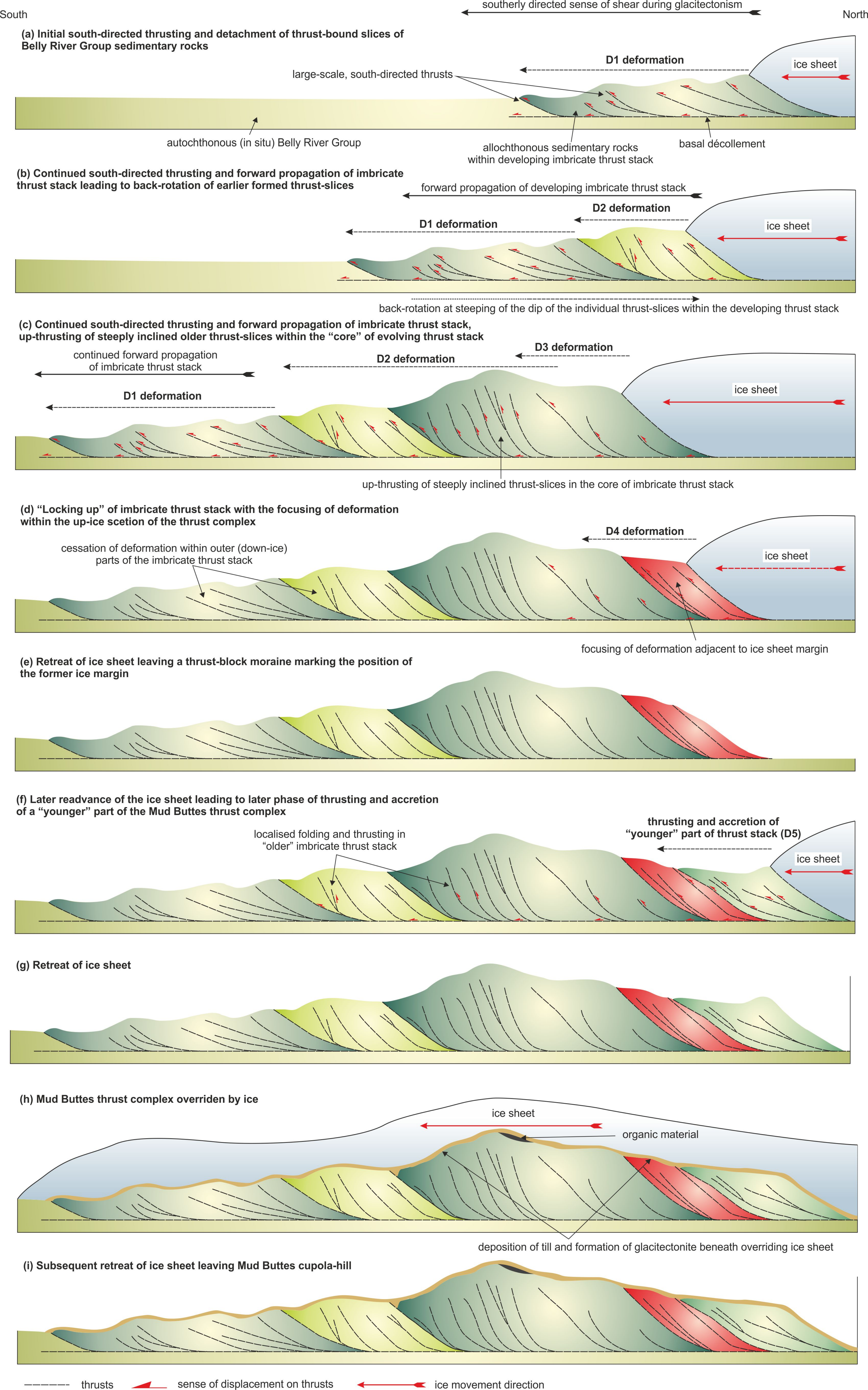
South
southerly directed sense of shear during glacitectonism
North
(a) Initial south-directed thrusting and detachment of thrust-bound slices of Belly River Group sedimentary rocks
D1 deformation
ice sheet
large-scale, south-directed thrusts
autochthonous (in situ) Belly River Group
allochthonous sedimentary rocks within developing imbricate thrust stack
basal décollement
(b) Continued south-directed thrusting and forward propagation of imbricate thrust stack leading to back-rotation of earlier formed thrust-slices
forward propagation of developing imbricate thrust stack
D2 deformation
D1 deformation
ice sheet
back-rotation at steeping of the dip of the individual thrust-slices within the developing thrust stack
(c) Continued south-directed thrusting and forward propagation of imbricate thrust stack, up-thrusting of steeply inclined older thrust-slices within the "core" of evolving thrust stack
continued forward propagation of imbricate thrust stack
D3 deformation
D2 deformation
D1 deformation
ice sheet
up-thrusting of steeply inclined thrust-slices in the core of imbricate thrust stack
(d) "Locking up" of imbricate thrust stack with the focusing of deformation within the up-ice scetion of the thrust complex
D4 deformation
cessation of deformation within outer (down-ice) parts of the imbricate thrust stack
ice sheet
focusing of deformation adjacent to ice sheet margin
(e) Retreat of ice sheet leaving a thrust-block moraine marking the position of the former ice margin
(f) Later readvance of the ice sheet leading to later phase of thrusting and accretion of a "younger" part of the Mud Buttes thrust complex
thrusting and accretion of "younger" part of thrust stack (D5)
localised folding and thrusting in "older" imbricate thrust stack
ice sheet
(g) Retreat of ice sheet
(h) Mud Buttes thrust complex overriden by ice
ice sheet
organic material
deposition of till and formation of glacitectonite beneath overriding ice sheet
(i) Subsequent retreat of ice sheet leaving Mud Buttes cupola-hill
thrusts
sense of displacement on thrusts
ice movement direction